

#### **OPEN ACCESS**

EDITED BY Pura Alfonso.

Universitat Politecnica de Catalunya, Spain

Mero Yannah. Institut de Recherches Géologiques et Minières (IRGM). Cameroon Hafizullah Abba Ahmed, Modibbo Adama University of Technology

\*CORRESPONDENCE Rames Chauke.

School of Physical Sciences, Nigeria

⋈ rchauke@geoscience.org.za

RECEIVED 04 June 2025 ACCEPTED 11 August 2025 PUBLISHED 10 September 2025

Chauke R (2025) Geology and geochemical variations within the eastern Lebowa Granite Suite, Bushveld Igneous Complex, South Africa: insights from fractionation and hydrothermal interference. Front. Geochem. 3:1640841. doi: 10.3389/fgeoc.2025.1640841

#### COPYRIGHT

© 2025 Chauke. This is an open-access article distributed under the terms of the Creative Commons Attribution License (CC BY), The use, distribution or reproduction in other forums is permitted, provided the original author(s) and the copyright owner(s) are credited and that the original publication in this journal is cited, in accordance with accepted academic practice. No use, distribution or reproduction is permitted which does not comply with these

# Geology and geochemical variations within the eastern Lebowa Granite Suite, Bushveld Igneous Complex, South Africa: insights from fractionation and hydrothermal interference

Rames Chauke\*

Council for Geoscience, Pretoria, South Africa

The Lebowa Granite Suite (LGS), representing the youngest component of the Bushveld Igneous Complex (BIC) magmatism, is closely associated with numerous polymetallic mineralisation assemblages. The intrusion of the LGS was accompanied by both long-lived mineralising hydrothermal systems and the concomitant reactivation of regional faults, resulting in endogranitic and exogranitic mineralisation. Despite extensive studies on the mineralisation, classification, and geochemistry of the LGS as the host rock, the different facies of the LGS have not been extensively appraised to elucidate their petrological evolution from a pristine and barren state to differentiatedmetasomatised fertile phases that host polymetallic mineralisation. Hence, the current study investigated two drill cores within the eastern limb of the BIC. These cores were logged, and a total of 25 samples representing Nebo, Bobbejaankop, Klipkloof, and Lease granites were collected for petrography and whole-rock geochemical studies. The BHDD 003 drill is characteristic of Nebo granite: leucocratic, equigranular, and biotite-bearing with common perthitic alkalifeldspar and biotite minerals showing pervasive sericite and chloritic alterations, respectively. The 648 KS/1 drill intersected Bobbejaankop granite, principally hypidiomorphic, characterized by pervasive sericite and minor microcline alterations in addition to chloritized magmatic biotite and hornblende. The Bobbejaankop granite grades into Lease granite, a finegrained variety. The Klipkloof granite, generally microgranitic but often granophyric, caps the Bobbejaankop granite at the top. The geochemical results indicate that the Nebo, Bobbejaankop, Klipkloof, and Lease granites are ferroan, calcic to alkali-calcic, peraluminous A-type, and developed within intracratonic settings. The Bobbejaankop granite shows evidence of higher fractionation than the Nebo granite, with evidence of intensive magmatichydrothermal alterations revealed by TEDI (Ba x (Sr/Rb)), Zr/Hf vs Y/Ho, Nb/Ta ratios, and normalised REE plots. Furthermore, the Bobbejaankop, Klipkloof, and Lease granites possess lower Zr/Hf (<~25), indicative of higher hydrothermal affluence and consequently a higher fertility index than the Nebo granite, implying that the former granites are more likely to host endogranitic polymetallic deposits. Normalised La/Yb ratios indicate that the facies of the

LGS are also cogenetic, likely emanating from the differentiation of mantle-derived alkaline mafic magma, similar to RLS, which is dominated by the removal of alkalis via subsolidus hydrothermal alteration processes.

**KEYWORDS** 

Lebowa Granite Suite, peraluminous A-type, petrogenesis, hydrothermal interference, fractionation

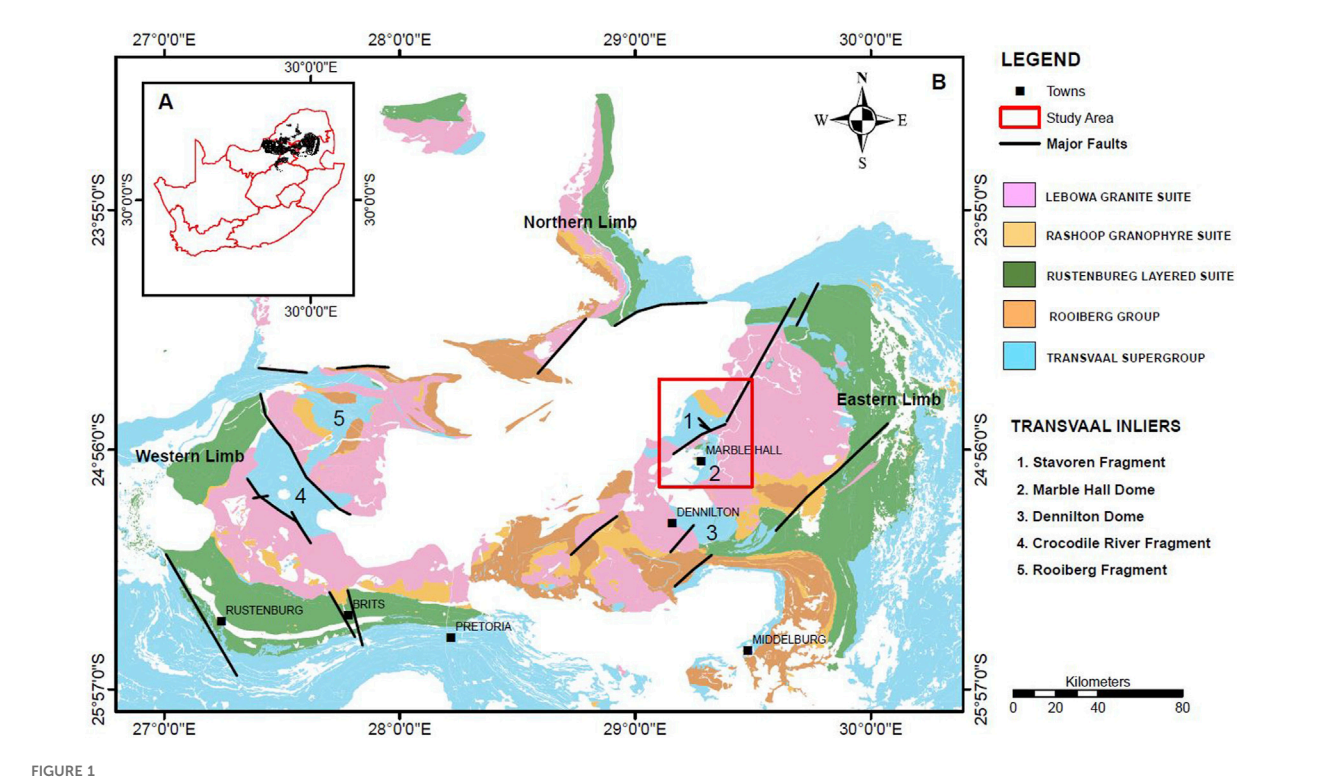
### 1 Introduction

The Lebowa Granite Suite (LGS) (c.2054.53 ± 0.59 Ma, CA-TIMS U-Pb age-Scoates et al., 2021), representing the youngest component of the Bushveld Igneous Complex (BIC), is closely with numerous polymetallic mineralization assemblages (Freeman, 1998; Robb et al., 2000). The intrusion of the LGS into earlier components of BIC magmatism and the Transvaal Supergroup was accompanied by both long-lived mineralizing hydrothermal systems and the reactivation of regional faults that facilitated endogranitic magmatic and magmato-hydrothermal, structurally controlled exogranitic mineralization (Pollard et al., 1991; McNaughton et al., 1993; Robb et al., 2000). The polymetallic mineralisation comprises an extended suite from orthomagmatic (Sn-Mo-W), through intermediate-mesothermal (Pb-Zn-Cu-As-Au-Ag), epithermal (Fe-F-U-REE) assemblages (Robb et al., 2000). These LGS polymetallic assemblages are unique and represent a complete evolution sequence of a magmatic-hydrothermal mineralisation cycle, unlike other polymetallic deposits that represent a single hydrothermal phase, such as the hypothermal (Sn-Nb-Mo) and mesothermal (Pb-Zn-Cu) deposits of the Ririwai Complex granites in northern Nigeria and mesothermal (U-Th) and (REE-Y) in the Bokan Mountain Complex in the United States (Kinnaird et al., 1985; Dostal and Shellnutt, 2016; Kamaunji et al., 2024).

Extensive studies on LGS and associated polymetallic mineralisation have focused on the nature and sources of fluids that gave rise to the stretched paragenetic sequence (Wagner, 1921; Ollila, 1981; Pollard et al., 1991; McNaughton et al., 1993; Robb et al., 1994; Freeman, 1998; Mutele and Hunt, 2022). These studies distinguished a range of metal-ligand complexes representing orthomagmatic through mesothermal to epithermal precipitation temperatures that were magmatic, meteoric, and connate derived (Robb et al., 2000 and references therein). Well-documented prominent tin and fluorite deposits representing orthomagmatic type (Sn-F-(W-Mo)) include, among others, Zaaiplaats tin (Pollard et al., 1989; Pollard et al., 1991; McNaughton et al., 1993; Vonopartis et al., 2020), Vergenoeg fluorite (Crocker, 1986), and Rooiberg tin (Stear, 1977; Ollila, 1981; Rozendaal et al., 1986; Rozendaal et al., 1995). The orthomagmatic Zaaiplaats tin deposit is characterised by an in situ fractional crystallisation of differentiated granites resulting in disseminated and low-grade mineralisation. Higher-grade mineralisation occurs in pipelike bodies in which cupola fluids fractured the granite rock to form lode-like deposits (Pollard et al., 1989). The Vergenoeg fluorite and Rooiberg tin deposits are also indirectly associated with these differentiated granites, where the metal fluid was likely sequestrated and percolated through the granite rocks to the intruded roof-rocks. Prominent discoveries of base metals typifying mesothermal and structurally controlled deposits include Spoedwel copper (Scoggins, 1991), the Houtenbek molybdenum deposit, and the Albert silver mine (Robb et al., 1994). These deposits are classified as vein-type mineralisation and are characterised by a transition from magmatic to magmatic-hydrothermal and/or mixing with connate fluids (Crocker et al., 2001; Kinnaird et al., 2004).

The petrogenesis of the LGS and the genetic relationships amongst the various granitic facies of the LGS remain the subject of much controversy after decades of Bushveld granites research and their associated polymetallic deposits (Robb et al., 1994; Freeman, 1998; Bailie and Robb, 2004). Hill et al. (1996), using both wholerock geochemistry data and Rb-Sr and Sm-Nd isotopes, suggested that partial melting of the Archaean quartzofeldspathic crystalline rocks by earlier mafic components of the BIC gave rise to the LGS. Their petrogenetic model employed O-isotopes and attributed geochemical variations in various facies of the LGS partly to regional variation of the composition in melted continental crust remnants. Based on whole-rock geochemistry, Kleemann and Twist (1989) are of the view that the differentiated nature of the LGS with stratigraphic height occurred through in situ fractionation, with a late-stage accumulation of magmatic fluids giving rise to hydrothermally altered granite facies. The crystallization models proposed by Coetzee and Twist (1989) and Hill et al. (1996) indicate that hydrothermally altered granites occur within the pluton, not solely in the apical portions. In the western limb of the LGS, Mutele and Misra (2021) observed concentric crystallization and magmatic liquid build-up towards the centre of the pluton. Fourie and Harris (2011) proposed, based on whole-rock Nd- and O-isotope data, that the LGS emanated from both fractional crystallization of mafic BIC components and partial assimilation of the crustal materials. Various studies (Kleemann, 1985; Coetzee and Twist, 1989; Pollard et al., 1991; Vonopartis et al., 2020) have suggested that the Bobbejaankop granites emanated from both fractional crystallisation and hydrothermal alteration of the Nebo granite. Other petrogenetic models maintain that the Bobbejaankop granite represents hydrothermally altered apical portions of the Nebo granite (Kleemann and Twist, 1989; McNaughton et al., 1993; Hill et al., 1996; Wilson et al., 2000; Kinnaird et al., 2004; Mutele and Misra, 2021).

Despite extensive literature maintaining that the Bobbejaankop granite is a magmatic-hydrothermal altered variant of the Nebo granite, there is negligible geochemical evidence supporting the assertion. In addition, a plethora of studies on the LGS have the focused on nature of the mineralising magmatic-hydrothermal fluids and classification of such polymetallic deposits. (e.g., Pollard and Taylor, 1986; McNaughton et al., 1993; Freeman, 1998; Robb et al., 2000; Bailie and Robb, 2004) There are few studies that holistically compare geochemical compositions and isotopes of the LGS plutons to explain their origin, detailing their petrogenesis and petrological evolution from pristine-barren state to differentiated-



(A) Map of South Africa showing provincial boundaries and aerial extent of the Bushveld Igneous Complex. (B) Geological map of the Bushveld Igneous Complex within the Transvaal Supergroup and its inliers. Inliers 1 and 2 denote the Stavoren Fragment and Marble Hall Dome, respectively, and occur adjacent to the study area enclosed within the red polygon (red box) enlarged in Figure 2. The rest of the Transvaal Supergroup inliers are numbered 3–5 (reproduced using Council for Geoscience 1:250,000 geological map).

metasomatized fertile phases with mineralising fluid (Kleemann and Twist, 1989; Coetzee and Twist, 1989; Hill et al., 1996; Mutele and Hunt, 2022). Therefore, the current study probes and compares the geochemical variations with the stratigraphic height of the basal Nebo granite in the Boschhoek Prospect and the overlying Bobbejaankop granite and associated Klipkloof and Lease granites from the Mutue Fides-Stavoren Tin field using whole-rock geochemistry from drill cores. The study also aims to determine the influence of hydrothermal alteration in the petrogenesis of the Bobbejaankop, Klipkloof, and Lease granites. Petrographic and geochemical characteristics of the Nebo, Bobbejaankop, Klipkloof, and Lease granites are presented here, focusing on differences brought upon by in-situ hydrothermal interference. The study of the geology, geochemistry, and genesis of the LGS is based on geological mapping and drill core logging combined with petrographic descriptions and whole-rock XRF major and ICP-MS trace element data of the Nebo and its differentiated mineralised varieties. It is supplemented by the historical stable isotopic data review of Fourie and Harris (2011). The study will provide insight into the evolutionary paths of an intrinsic Nebo granite facies and the possible facies that it may evolve into as a function of magma composition and magmatichydrothermal processes that constitute LGS.

# 2 Geological settings

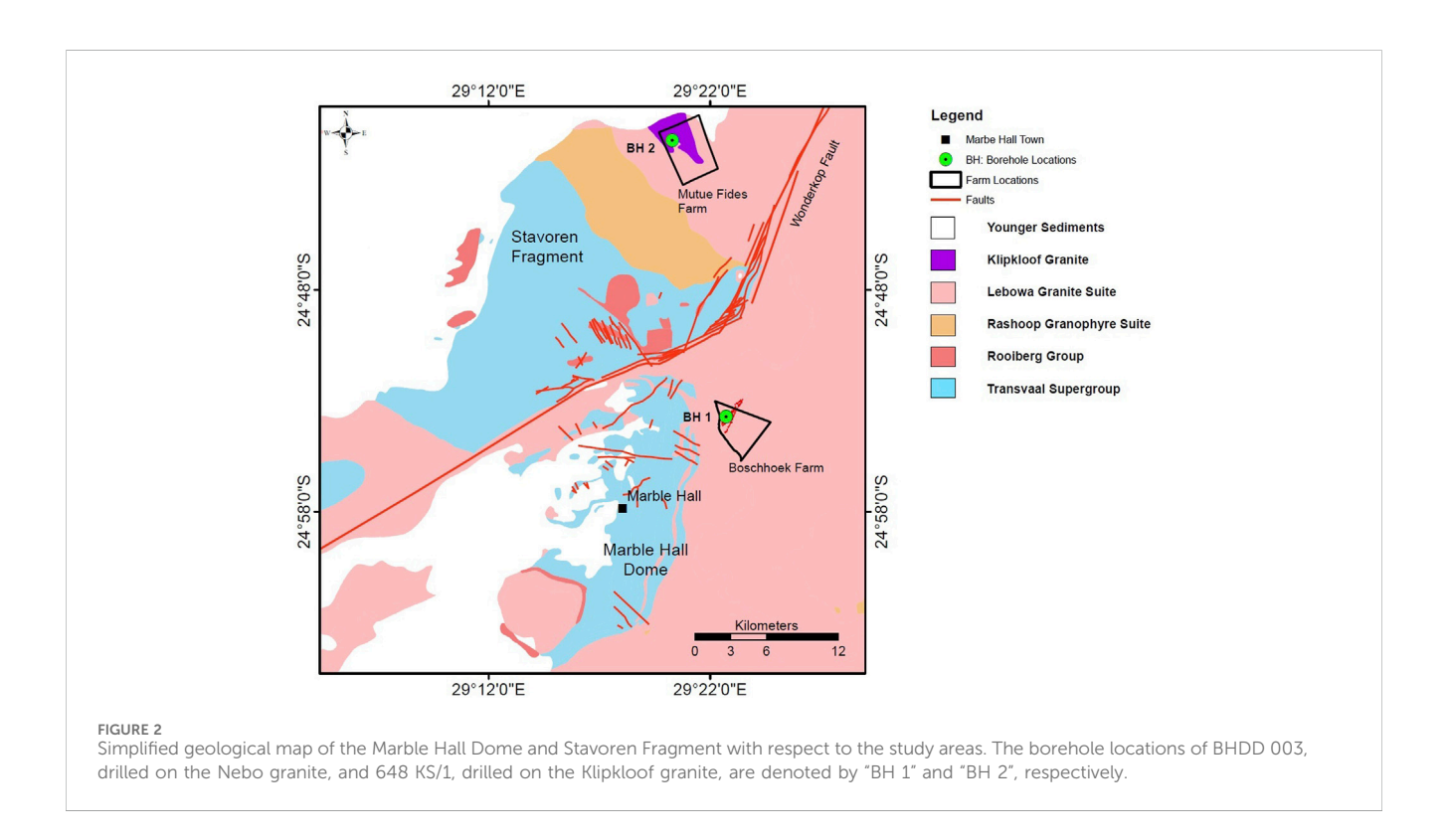
The Bushveld Igneous Complex (BIC) is a large igneous province (LIP) that comprises the earlier extrusive and bimodal

Rooiberg Group (2057.3 ± 3.8 Ma; Harmer and Armstrong, 2000), the ultramafic and mafic Rustenburg Layered Suite (RLS) (2055.91  $\pm$ 0.26 Ma, CA-ID-TIMS age; Zeh et al., 2015), the Rashoop Granophyre Suite (RGS), and the felsic Lebowa Granite Suite (Cawthorn et al., 2006) (Figure 1). The BIC intruded the Archaean to Proterozoic (2,670-2060 Ma, Lu-Hf zircon; Zeh et al., 2016) siliciclastic and carbonate rocks of the Transvaal Supergroup deposited on the Archaean Kaapvaal Craton (Eriksson et al., 1995; 2006). It occupies over 350,000 km<sup>3</sup> and extends for 66,000 km<sup>2</sup> (Cawthorn and Walraven, 1998; Buick et al., 2001) (Figure 1). The RLS intrusion is preserved in five limbs: western, eastern, northern, southern (Bethal), and far-western (Groot Marico). The intrusion is between 7 and 9 km thick. It is generally accepted that the RLS intruded and cooled within 1 million years (Cawthorn and Walraven, 1998; Zeh et al., 2015). The layers of the RLS were proposed to be almost horizontal during formation; however, they now dip towards the centre of the intrusion (Gough and van Niekerk, 1959; Cawthorn and Walraven, 1998).

The intrusion of the LGS marked the last major magmatic event of the BIC and developed as a compositionally zoned sheeted body of A-type granites (Kleemann and Twist, 1989; Hill et al., 1996). The Bushveld granites, as they are colloquially known, developed a large, sheeted pluton with an estimated thickness of 2.5–3.5 km covering 30,000 km² (Molyneux and Klinkert, 1978; Kleemann and Twist, 1989). SACS (1980) recognised seven facies of the Bushveld granites: the Nebo, Klipkloof, Lease, Bobbejaankop, Sekhukhune, Verena, Balmoral, and Makhutso granites (MacCaskie, 1983; Ferré et al., 1999; Wilson et al., 2000). The Nebo granite is the most common

TABLE 1 LGS facies in the eastern Limb of BIC and their respective characteristics (after MacCaskie, 1983; Kleemann and Twist, 1989).

Granite facies (subtypes)	Characteristics
Lease granite	Grey to pink, aplitic microgranite, transitional contacts with Bobbejaankop and Klipkloof granites
Klipkloof granite	Pink, medium to fine-grained, sharp contacts with Nebo granite
Bobbejaankop granite	Pink to brick red, coarse to medium, sharp contacts with granophyre and transitional with Nebo granite
Nebo granite (Sekhukhune, Verena, Makhutso)	Grey to pale pink, coarse to very coarse-grained, sharp contacts with rhyolite and transitional with granophyre



type and is often crosscut and graded into other facies. The aplitic Klipkloof and Bobbejaankop granites are distinguished by colour and texture and are also widespread across the complex (Kleemann and Twist, 1989). Other facies are restricted to specific locations and are consequently named after those areas (Crocker et al., 2001). Their respective appearances and contact relations with the surrounding rocks (MacCaskie, 1983; Kleemann and Twist, 1989) are shown in Table 1.

# 2.1 Local geology and field descriptions

The study areas cover the Boschhoek Prospect and Mutue Fides-Stavoren Tin Field and are respectively situated roughly 20 km northeast and 30 km north of Marble Hall Town in Limpopo Province (Figure 2). Both the Boschhoek Prospect and Mutue Fides-Stavoren Tin Field occur within the eastern limb of the BIC and are adjacent to the Transvaal Supergroup inliers separated by the Wonderkop Fault. The Nebo granite in the Boschhoek Prospect forms east-west low undulating domal hills crosscut perpendicularly by siderite-calcite-quartz veins

(MacCaskie, 1983). In some areas within the vicinity of the Prospect, the Nebo granite outcrops are often exfoliated and jointed, consistent with observations by MacCaskie (1983). The granite is typically pale pink, coarse-grained, and equiangular and chiefly consists of quartz, perthite, and hornblende (Kleemann and Twist, 1989; Evans, 2015). However, it also occurs as a greyish-brown, coarse-grained variety often surrounding the Boschhoek Prospect vein system (MacCaskie, 1983). Gossanous ridges, striking northeast to southwest, cap an array of veins (Smits, 1979; Evans, 2015). The veins, comprising siderite, pyrite, calcite, and quartz, exhibit a sigmoidal dextral wrench structure, referred to as "Boschhoek structure" and range from a few centimetres to tenths of metres in width (Evans, 2015) (Figure 2).

Within the Mutue Fides-Stavoren Tin Field study area, the main rocks are predominantly aplitic Lease granite and the porphyritic and fine-to medium-grained microgranitic Klipkloof variety (Crocker et al., 2001). Brick-red, medium-grained Bobbejaankop granite, referred to as "red granite" by Wagner (1921), also outcrops (Crocker et al., 2001). The historical Grass Valley tin mine at the Farm Mutue Fides mine is situated on this type of granite, and quite often these Bobbejaankop granite outcrops are hydrothermally

altered (Crocker et al., 2001). Granophyric granite, resembling the Klipkloof granite, rarely outcrops within the Mutue Fides mine but is common on Stavoren farm and adjacent farms such as Arcadia farm (Wagner, 1921). Underground mining reports and field observations from the mined-out material show that all these granite facies are also crosscut by pegmatitic veins comprising k-feldspar and quartz and tin-base metal mineralisation (Crocker et al., 2001).

The Mutue Fides farm comprises predominantly aplitic Lease granite that is occasionally porphyritic and the fine-to medium-grained microgranitic Klipkloof granite (Crocker et al., 2001). Brick-red medium-grained Bobbejaankop granite, Wagner's "red granite", frequently outcrops at Mutue Fides (Wagner, 1921; Crocker et al., 2001). The historical Grass Valley mine at Mutue Fides mine was situated on this type of granite, and quite often these Bobbejaankop granite outcrops are weathered (Crocker et al., 2001). Granophyric granite, resembling the Klipkloof granite, seldom outcrops at Mutue Fides, but prominent outcrops are found on the Stavoren and adjacent farms such as Arcadia farm (Wagner, 1921). Underground mining reports and field observations from the mined-out materials show that all these granite facies possess pegmatite veins comprising k-feldspar and quartz and are mineralised in some cases (Crocker et al., 2001).

# 3 Sampling and analytical methods

The study considered two 5-cm diameter diamond drill cores: BHDD 003 (BH 1) from Boschhoek farm 752 KS within the Boschhoek Prospect extending for an apparent depth of 350 m drilled in 2010, and 648 KS/1 (BH 2) from Mutue Fides farm 648 KS located within the Stavoren-Mutue Fides Tin Field with 195 m depth and drilled in the 1970s (Figure 2). These drill cores were logged to characterise both their mineralogy and its chemical alteration. BHDD 003 crosscut the Nebo granite encountered during field mapping and was consistent with the description by Kleemann and Twist (1989) and Evans (2015). The 648 KS/1 drill intersected mainly the Bobbejaankop granite, resembling the facies first described by Wagner (1921) as "red granite". At depths, the Bobbejaankop granite grades into porphyritic Lease and granophyric Klipkloof granites. The Lease and Klipkloof granites were also encountered in the Stavoren-Mutue Fides tin field during field mapping and were identified using descriptions by Crocker et al. (2001) as a reference. The complete logs and sampled location points are contained in my thesis (Chauke, 2022). For the current study, six pristine core samples from BHDD 003 and 19 samples from 648 KS/1 between 12 cm and 35 cm long were sampled and split before preparation for geochemical analyses at the Council for Geoscience, Pretoria. The samples were cleaned using high-pressure water and then air-dried before being crushed to 5 mm in a carbonsteel jaw crusher. Subsequently, they were split and milled to less than 75-µm sieve size using an aluminium ring mill and transported to the University of the Witwatersrand, Johannesburg for analysis.

From the 648 KS/1 core, 19 samples were partitioned into five samples representing Bobbejaankop granite, six representing aplitic Klipkloof granite, and eight representing microgranite Lease granite. Collectively, these samples are termed "Bobbejaankop-like granite" for better comparison with the Nebo granite.

The concentrations for the whole-rock major and minor elements were determined using a wavelength-dispersive (WD) X-ray fluorescence (XRF-Panalytical) instrument at the Earth Lab, University of the Witwatersrand (Johannesburg). Calibration standards were obtained from the International Reference Materials USGS series (United States) and NIM series (South Africa). The Earth Lab also analysed the trace element, including rare earth element (REE), concentrations using a quadrupole Induced Coupled Plasma Mass Spectrometry (ICP-MS Perkin Elmer Elan DRC-e) instrument. AGV-2, BCR-1, and BR-1 International reference materials were used as calibration standards. The REE and incompatible trace elements were normalised using chondrite and primitive mantle values, respectively, from Sun McDonough (1989).

# 4 Petrographic descriptions

#### 4.1 Nebo granites

The equigranular-Nebo granite generally comprises subhedral, coarse-grained (1-6 mm) perthitic k-feldspar (60%), subhedral to anhedral quartz grains (0.5 mm-2 mm; 30%), and plagioclase (0.5-1.5 mm; 5%). Minor anhedral biotite and hornblende (both constitute ~5%) fill interstitial spaces (<0.5 mm in size). Almost all plagioclase grains are surrounded by perthite and other k-feldspars. These plagioclase grains are characterised by polysynthetic twinning and exhibit minor sericite alterations (Figures 3A,B). In rare cases, perthite exhibits irregular intergrowths of albite and orthoclase that form patches or lenses. Perthite and quartz grains formed clusters characterised by a synneusis texture, with the latter grains showing undulose extinction signalling strain (Figure 3C). Some quartz grains were annealed and sutured along the grain boundaries (Figure 3C). These sutured grain boundaries often possess fluid inclusions and opaque minerals. Obliterated plagioclase and biotite form sericite, together with chlorite and muscovite, collectively forming a saussurite assemblage (Figure 3D). Biotite and, to a lesser extent hornblende, form clusters and fill interstitial spaces between k-feldspar grains (Figure 3E). These grains are chloritized in some cases. The chloritization in biotite mainly occurs along the cleavage planes and often exhibits inclusions of quartz and opaque minerals (Figure 3F). Other accessory minerals include zircon, apatite, and rutile. The zircon crystals are typically euhedral.

#### 4.2 Bobbejaankop granites

The Bobbejaankop granite comprises subhedral-to-anhedral k-feldspar (0.5–5 mm, 40%) and plagioclase (0.5–1 mm, 25%) and subhedral-to-anhedral quartz grains (0.5–2 mm, 30%), with anhedral, chloritized biotite (<0.5 mm, 5%) filling interstitial spaces. The k-feldspars are predominantly perthitic (0.5–2 mm), exhibiting patchy and irregular intergrowth textures. The plagioclase shows polysynthetic twinning and is often sericitized, resulting in micaceous aggregates. The plagioclase often appears exsolved within the perthite grains, exhibiting patchy characteristics (Figures 4A,B). The microclinised plagioclase variants appear brown with a black tint owing to the colouration of the Fe

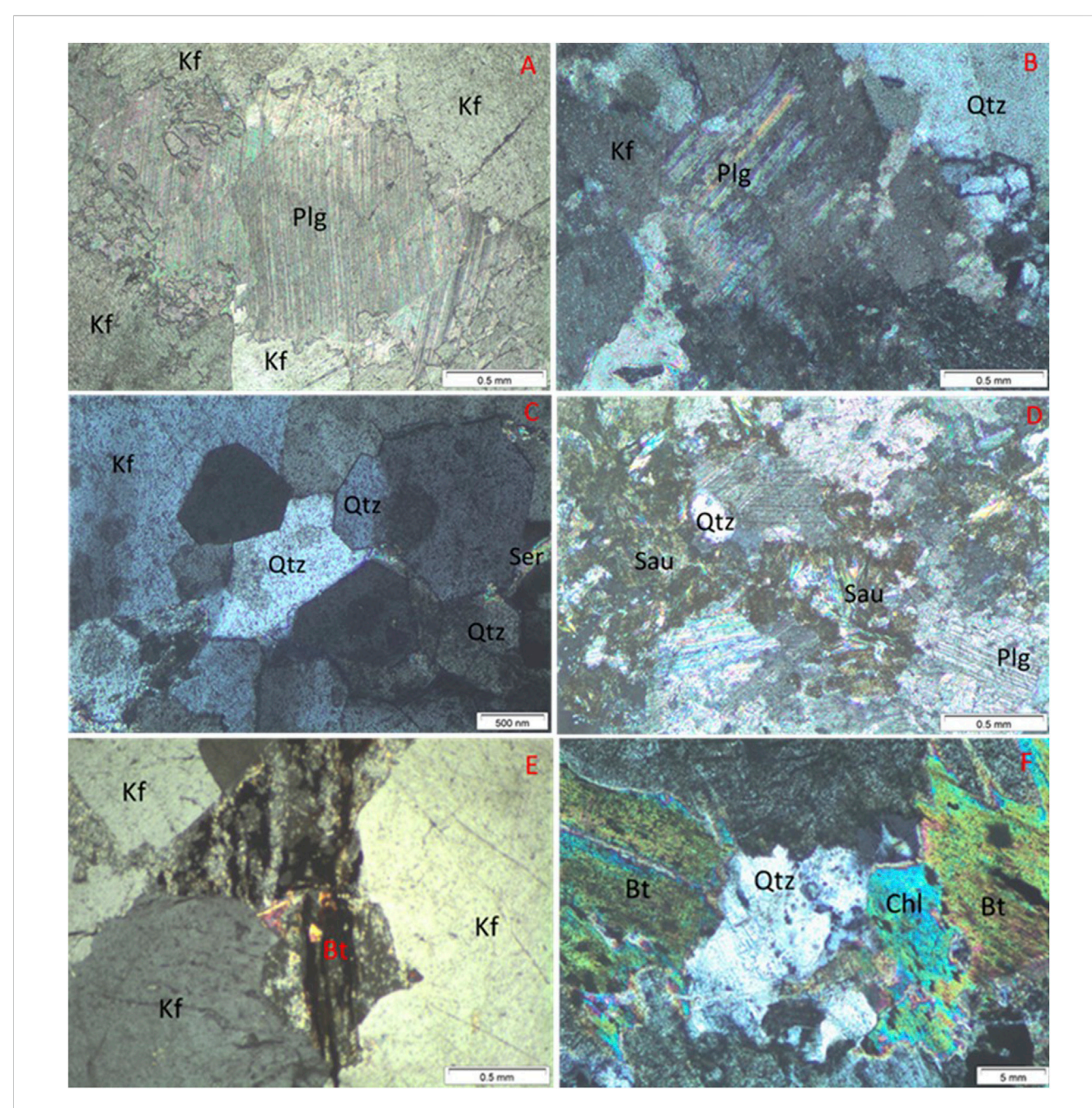


FIGURE 3
Photomicrographs taken in XPL of Nebo granite from the BHDD 003 core. (A) Plagioclase (Plg) grains surrounded by k-feldspars (Kf), sampled at a depth of 14.66 m, sample RCB 03. (B) Selective alteration of plagioclase (Plg) to sericite, leaving behind quartz (Qtz) and k-feldspar (Kf). Sampled at a depth of 137.60 m, sample RCB 04. (C) Annealed quartz grains along boundaries exhibiting undulose extinctions, sampled at a depth of 137.60 m, sample RCB 04. (D) Altered plagioclase (Plg) and saussurite (Sau) assemblages, sampled at a depth of 137.60 m, sample RCB 04. (E) Biotite (Bt) clusters surrounded by k-feldspars (Kf) sampled at a depth of 18 m, sample RCB 01. (F) Extensive biotite (Bt) alteration to chlorite (ChI), sampled at a depth of 18 m, sample RCB 01.

coating, a phenomenon attributed to hematite formation due to fluid-rock interaction (Figure 4D). The quartz grains exhibit granular, hypidiomorphic, and synneusis-textures (Figure 4A).

#### 4.3 Lease granites

The Bobbejaankop granite in the 648 KS/1 drill hole grades into fine-to medium-grained Lease granite. The Lease granite exhibits

holocrystalline, largely seriate with porphyritic textures comprising k-feldspar (50%), quartz (40%), plagioclase (5%), and lesser biotite and hornblende (constitutes less than 5%) filling interstitial spaces. The porphyritic portions are characterised by k-feldspar and quartz phenocrysts (2–5 mm) exhibiting euhedral textures included within a 0.1–1 mm fine-grained groundmass. These phenocrysts of k-feldspar and quartz crystals also exhibit poikilitic textures. The Lease granite shows similar mineral abundances to the Nebo granite; however, the latter possesses more quartz crystals and less biotite and hornblende.

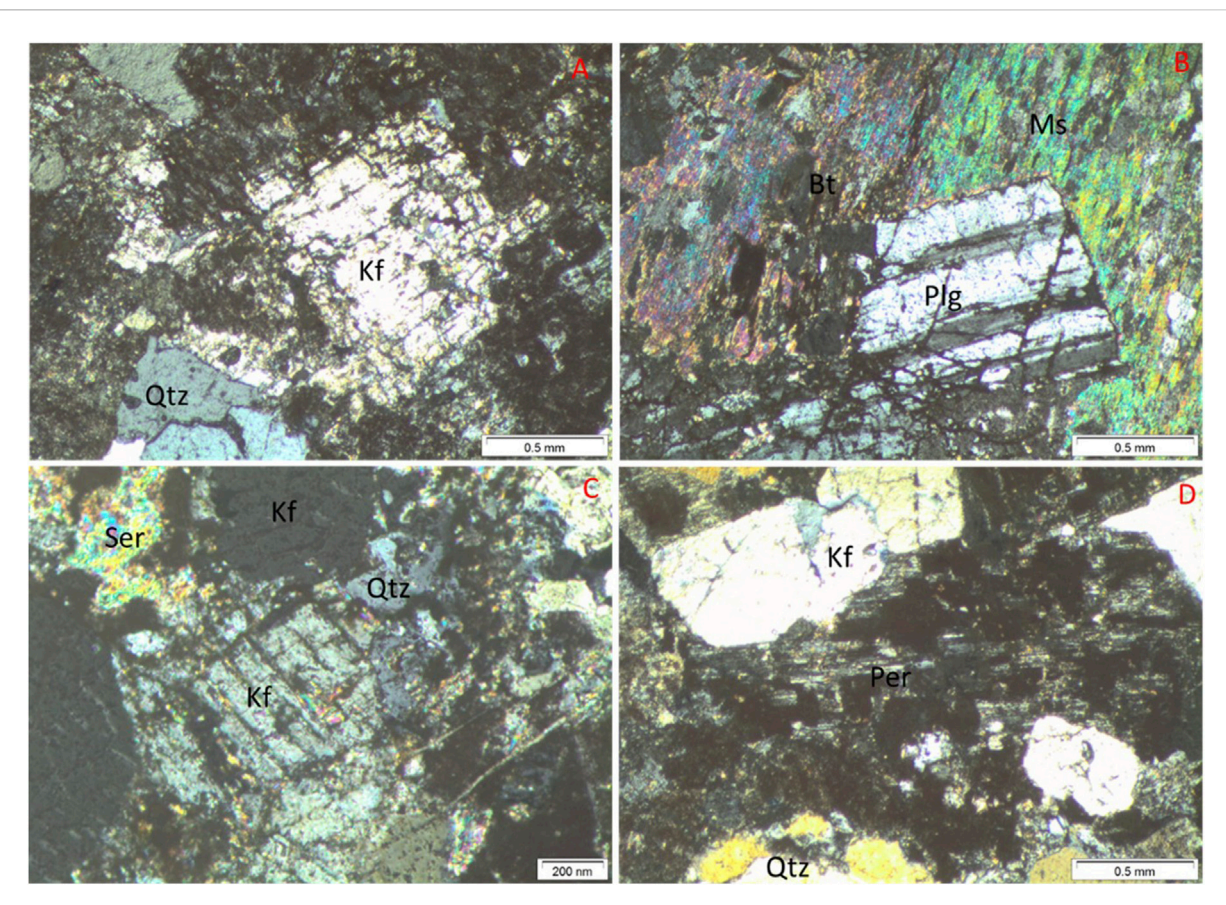


FIGURE 4
Photomicrographs from 648 KS/1 core taken in XPL. (A) Patchy and irregular k-feldspar (Kf) and synneusis-textured quartz (Qtz) grains, sampled a depth of 10.28 m, sample RCM 01. (B) Typical polysynthetic twinning by plagioclase (Plg) often altered to micaceous aggregates, sampled at a depth of 10.28 m, sample RCM 01. (C) Patchy and chessboard-like texture of k-feldspar, altered to sericite (Ser), sampled at a depth of 19.95 m, sample RCM 02. (D) Altered perthite matrix within k-feldspar and quartz phenocrysts, sampled at a depth of 19.95, sample RCM 02.

#### 4.4 Klipkloof granites

The granophyric Klipkloof granites form part of the uppermost portions of the core. The fine-grained to medium-grained microgranite shows gradational contact with both Bobbejaankop and Lease granites. The Klipkloof granite comprises subhedral k-feldspar (0.2–1 mm, 40%), anhedral quartz (0.2–1 mm, 35%), plagioclase (0.1–1 mm, 15%), and lesser subhedral-to-anhedral interstitial biotite and chlorite (0.2–5 mm, both 10%). Perthitic k-feldspar and quartz exhibit graphical intergrowths. K-feldspar shows patchy and chessboard-like exsolutions, which in some cases are intensively altered to sericite (Figure 4C). Biotite is partly altered to chlorite but often completely to sericite, following a biotite, sericite-to-chlorite paragenesis.

#### 4.5 Alteration phases

The granites studied possess similar mineralogies and alteration assemblages, albeit different textures and variable alteration degrees. Generally, two main alteration phases are observed in all the studied granites: the pervasive alteration of feldspars to sericite and an extensive chloritization of biotite. Biotite also alters to fine-grained muscovite in Bobbejaankop granites. In Bobbejaankop granites and associated

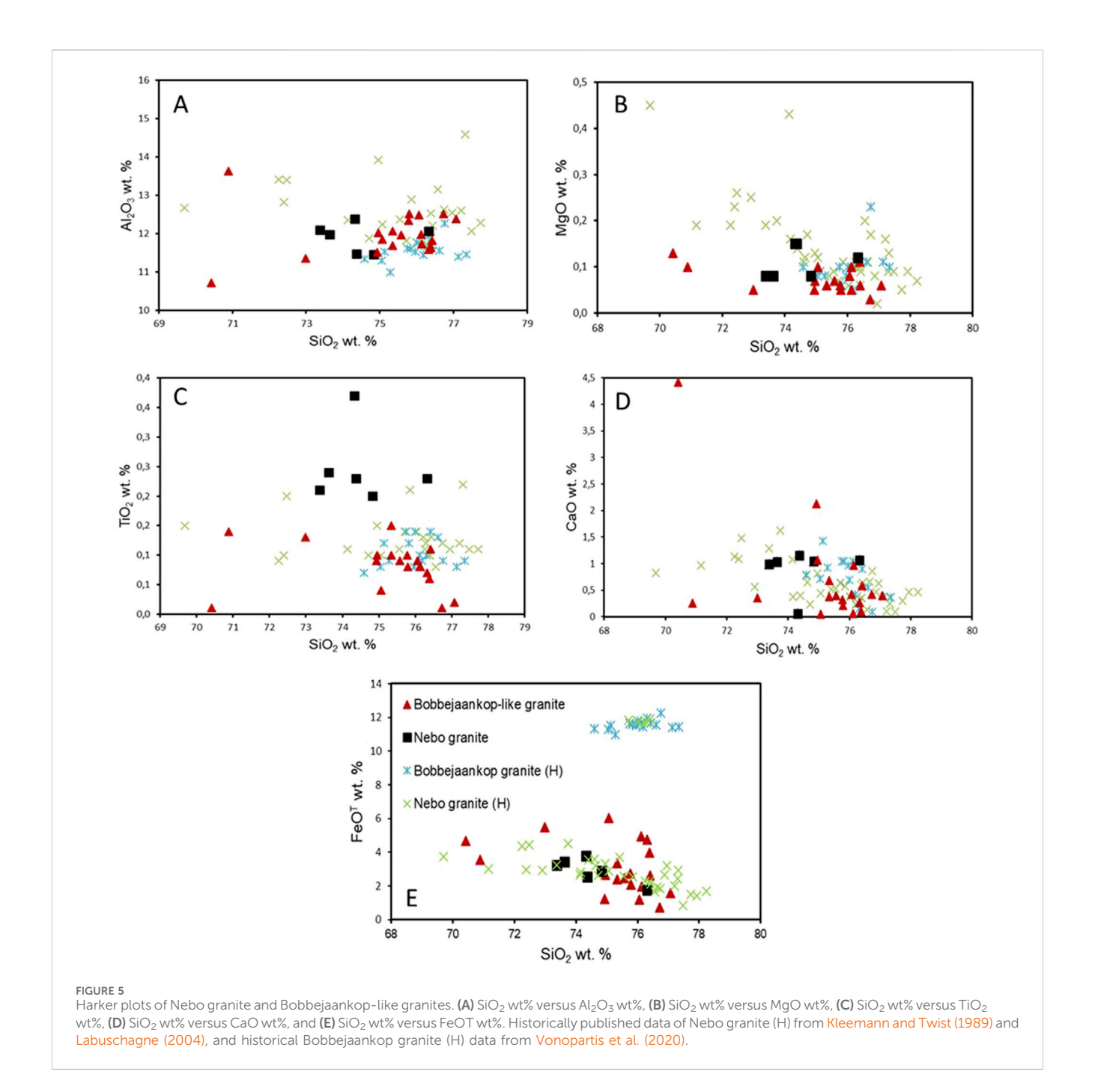
Klipkloof and Lease granites, perthite seldom exhibits partial microclinisation. The Lease granite, in addition to the main alteration phases, exhibits patches of epidotisation. The sericitization of perthite often precedes chloritization, which in turn is followed by microclinisation. It is unclear which alteration phase precedes the other between microclinisation and epidotisation.

# 5 Whole-rock geochemistry of granites

The geochemical variations of drill core samples are modelled as a function of magmatic fractionation and hydrothermal alterations and subsequently imply their petrogenetic evolution, possible cogenesis, and fertility, showing characteristic alteration signatures indicative of mineralisation. The whole-rock major element and trace element concentrations are presented in Supplementary Tables S1 and S2.

# 5.1 Major element geochemistry

The ranges and averages of major elements are consistent with the reported general geochemical concentration of the LGS



(Kinnaird et al., 2004). The Nebo and the Bobbejaankop-like granites contain high  $SiO_2$  concentrations of 70.42–77.06 wt% (n = 6) and 73.63–76.32 wt% (n = 19), respectively (Supplementary Table S1). Both granite types contain low concentrations of CaO, ranging between 0.04 wt% and 4. wt%, averaging 1 wt% (n = 25). The MgO and  $P_2O_5$  concentrations are extremely low in both granites, <0.15 wt% and 0.04 wt%, respectively. The averages of  $K_2O$ ,  $Na_2O$ , and their ratios ( $K_2O/Na_2O > 1$ ), MgO, and  $P_2O_5$  contents are typical signatures for A-type granites (Whalen et al., 1996; King et al., 1997; Kleemann and Twist, 1989). The Fe content and FeO/MgO ratio also indicate their A-type ferromagnesian nature (Kleemann and Twist, 1989). Bivariate plots of some major oxides representing unaltered samples are presented in Figure 5.

The Fe-index (Fe\* = FeOT/(FeOT + MgO)) in both the Nebo and the Bobbejaankop-like granites satisfy the condition (FeOT/(FeOT + MgO) > 0.486 + 0.0046 × wt% SiO<sub>2</sub>) to be regarded as ferroan A-type granites after the discrimination diagram of Frost et al. (2001) and Frost and Frost (2008) (Figure 6A). The Alumina Saturated Index (ASI) represented by molar (Al<sub>2</sub>O<sub>3</sub>/(CaO + Na<sub>2</sub>O + K<sub>2</sub>O)), also known as the "Shand Index" (Shand, 1922; Maniar and Piccoli, 1989), ranges from 1.58 to 3.67, suggesting that these A-type granites are peraluminous (Figure 6B). These suites are sub-alkaline with calc-alkalic to calcic composition, as indicated in the Modified Alkali Lime Index (MALI) diagram (Frost et al., 2001) (Figure 6C). The Nebo granite samples mainly plot within the calc-alkalic field extending from the calcic field. The Bobbejaankop-like granite

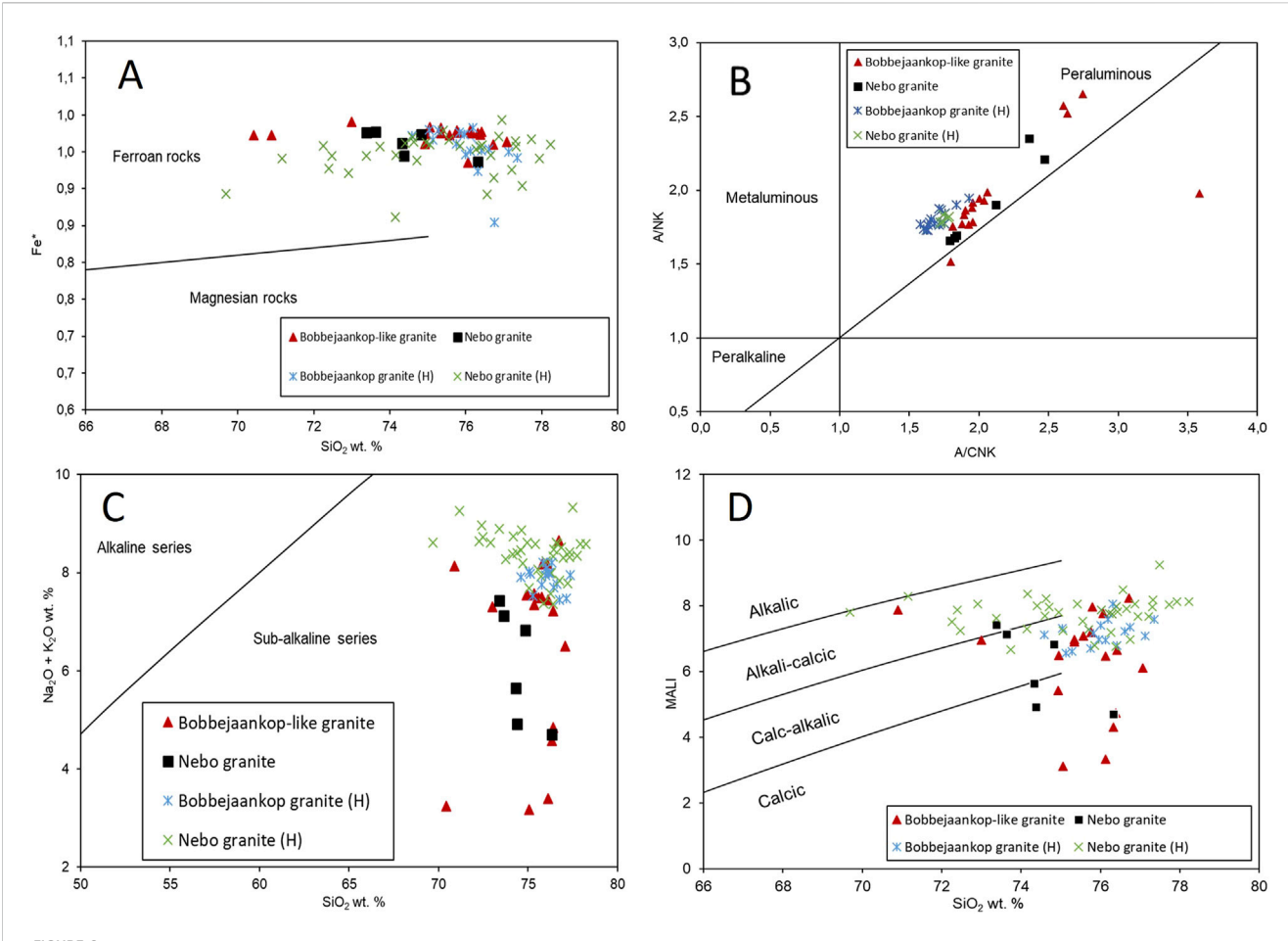


FIGURE 6
(A) Fe\* versus  $SiO_2$  plot depicting the Ferroan nature of the Nebo granite and Bobbejaankop-like granites. Fe\* =  $FeO^T/(FeO^T + MgO)$  (after Frost and Frost, 2008). (B) ASI discrimination plot classifying the Nebo granite and Bobbejaankop-like granite as peraluminous granites. A/CNK = molar  $Al_2O_3/(CaO + Na_2O + K_2O)$ ; A/NK = molar  $Al_2O_3/(Na_2O + K_2O)$  (after Maniar and Picooli, 1989). (C) Alkalinity discrimination diagram affirming the sub-alkaline character of both Nebo and Bobbejaankop-like granite samples (after Irvine and Baragar, 1971). (D) MALI discrimination diagram describing the fractionation trends of Nebo and Bobbejaankop-like granite samples. MALI =  $Na_2O + K_2O + CaO$  wt% (after Frost et al., 2001). Historically published data of Nebo granite (H) from Kleemann and Twist (1989) and Labuschagne (2004), and historical Bobbejaankop granite (H) data from Vonopartis et al. (2020).

samples also extend from the calcic to calc-alkali field; however, they show a relatively wider spread than the Nebo granite (Figure 6D).

#### 5.2 Trace elements

The Nebo granite samples show high Rb (138–186 ppm; aver. 158 ppm (n = 6)), Th (19–30 ppm, aver. 24 ppm (n = 6)), and U (4–6 ppm, aver. 5 ppm (n = 6)) but relatively depleted Ba (475–935 ppm, aver. 776 ppm (n = 6)), Sr (17–69, aver. 41 ppm (n = 6)), and Zr (185–322 ppm, aver. 248 ppm (n = 6)). The Nebo granite also shows concentrations of compatible elements such as Cr, Co, Ni, and V, which is typical of the LGS (e.g., Kleemann and Twist, 1989). The Bobbejaankop-like granite samples show comparably higher concentrations of Rb (235–619 ppm, averaging 407 ppm (n = 19)), Th (3–75, averaging 32 ppm), and U (3–39 ppm, averaging 15 ppm) relative to the Nebo granite samples (Supplementary Table S2). The Bobbejaankop granites are also depleted in Ba (36–181, averaging 108 ppm), Sr (2–11 ppm, averaging 6 ppm), and Zr (165–878 ppm, averaging

360 ppm) compared to non-A-type granites (Kleemann and Twist, 1989). Both granites further show low concentrations of compatible elements such as Cr, Co, Ni, and V, which is typical of samples from the LGS (Kleemann and Twist, 1989).

Using the tectonic discrimination diagram (Pearce et al., 1984), the granite facies plot the "within plate granite" (WPG) field (Figure 7). In addition, using a discrimination diagram (Whalen et al., 1987), the Bushveld granites also show the affinity of an A-type granite (Figure 8A). Similarly, use of trace element ratios ratifies the A-type nature of the granites, as illustrated by the major element plots (Figure 8B). The Nebo granite shows Rb/Sr ratios of 2-11, whereas the Bobbejaankop-like granite shows relatively higher Rb/Sr ratios of 44-229. Higher Rb/Sr ratios may be indicative of the relatively higher fractionation of Bobbejaan-like granite facies relative to the Nebo granite (El Bouseily and El Sokkary, 1975). A trace element differentiation index (TEDI) (Walraven, 1986) is defined as Ba × (Sr/Rb), yielding values of 70-399 for Nebo granite and 0.1-4 for Bobbejaankop-like granite (Figure 9A). Higher values suggest the least fractionated magma product, and values lower than 10 imply a highly fractionated magma product (Bailie, 1997;

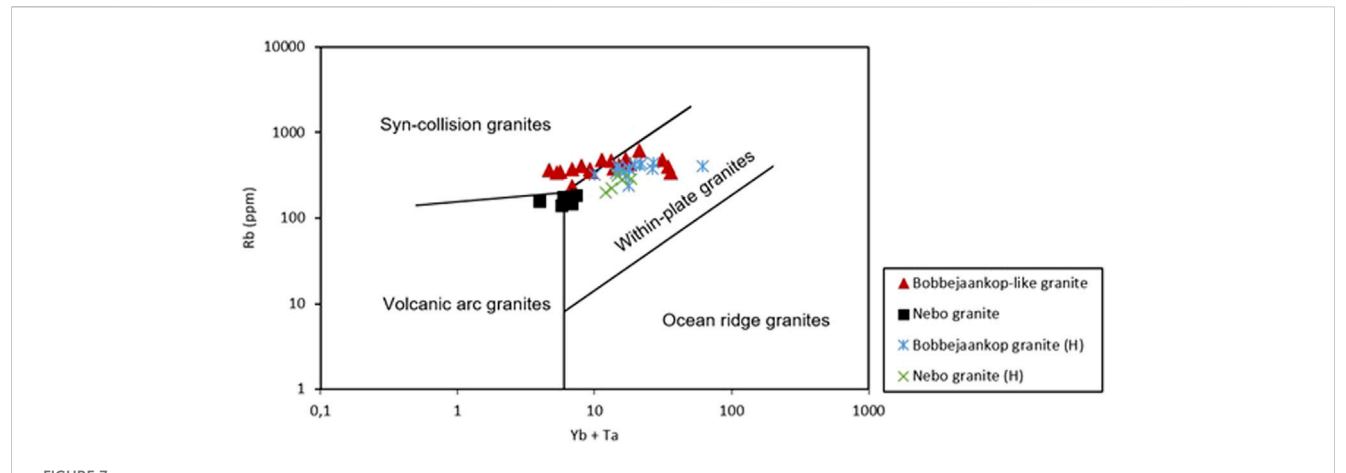
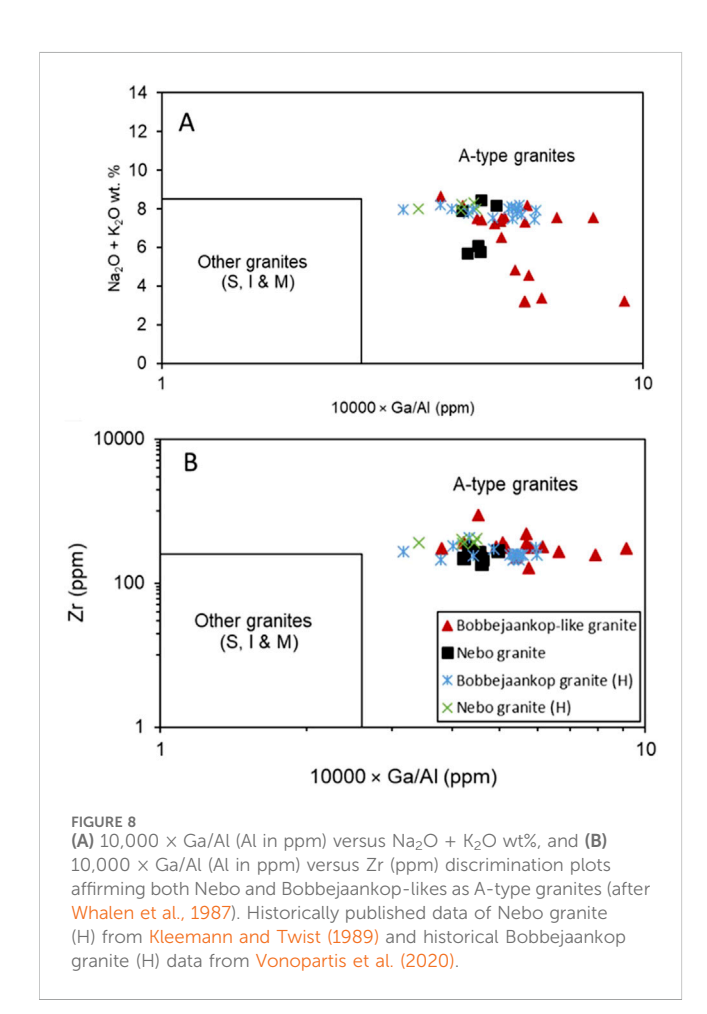


FIGURE 7
Rb versus (Yb + Ta) after Pearce et al. (1984), tectonic discrimination diagram of Nebo granite and Bobbejaankop-like granite plotting mainly "within-plate granites" field, with slight overlaps to volcanic arc granites and syn-collision granites, respectively. Historically published data of Nebo granite (H) from Kleemann and Twist (1989) and historical Bobbejaankop granite (H) data from Vonopartis et al. (2020).



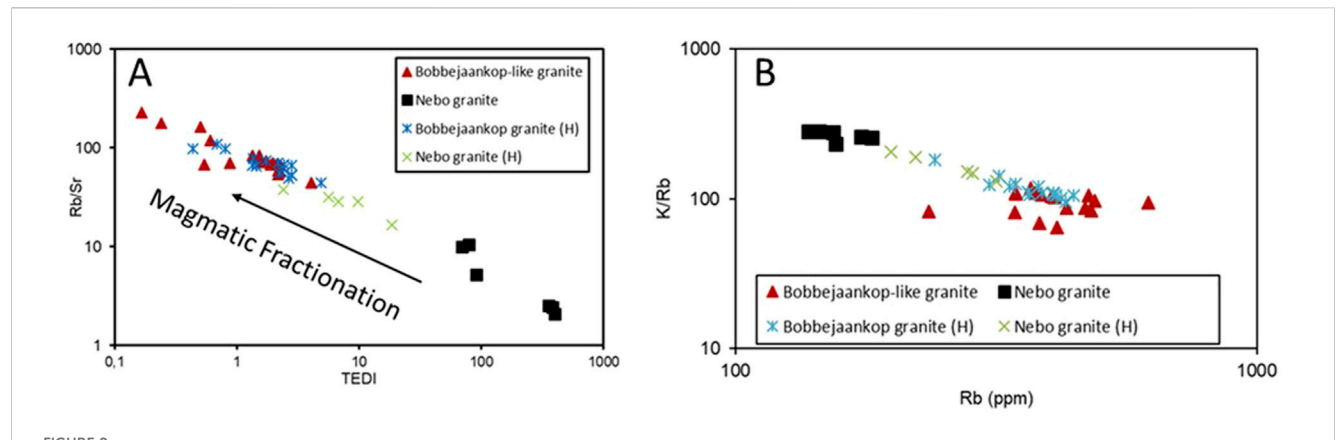
Freeman, 1998; Bailie and Robb, 2004). The Nebo granite depicts a K/Rb ratio of 231–283, whereas the Bobbejaankop-like granite shows a significantly lower ratio of 69–117. The lower Bobbejaankop-like granite K/Rb ratios suggest higher fractionation and, evidently, the influence of aqueous fluid (Shaw, 1968) (Figure 9B).

#### 5.3 Rare earth elements

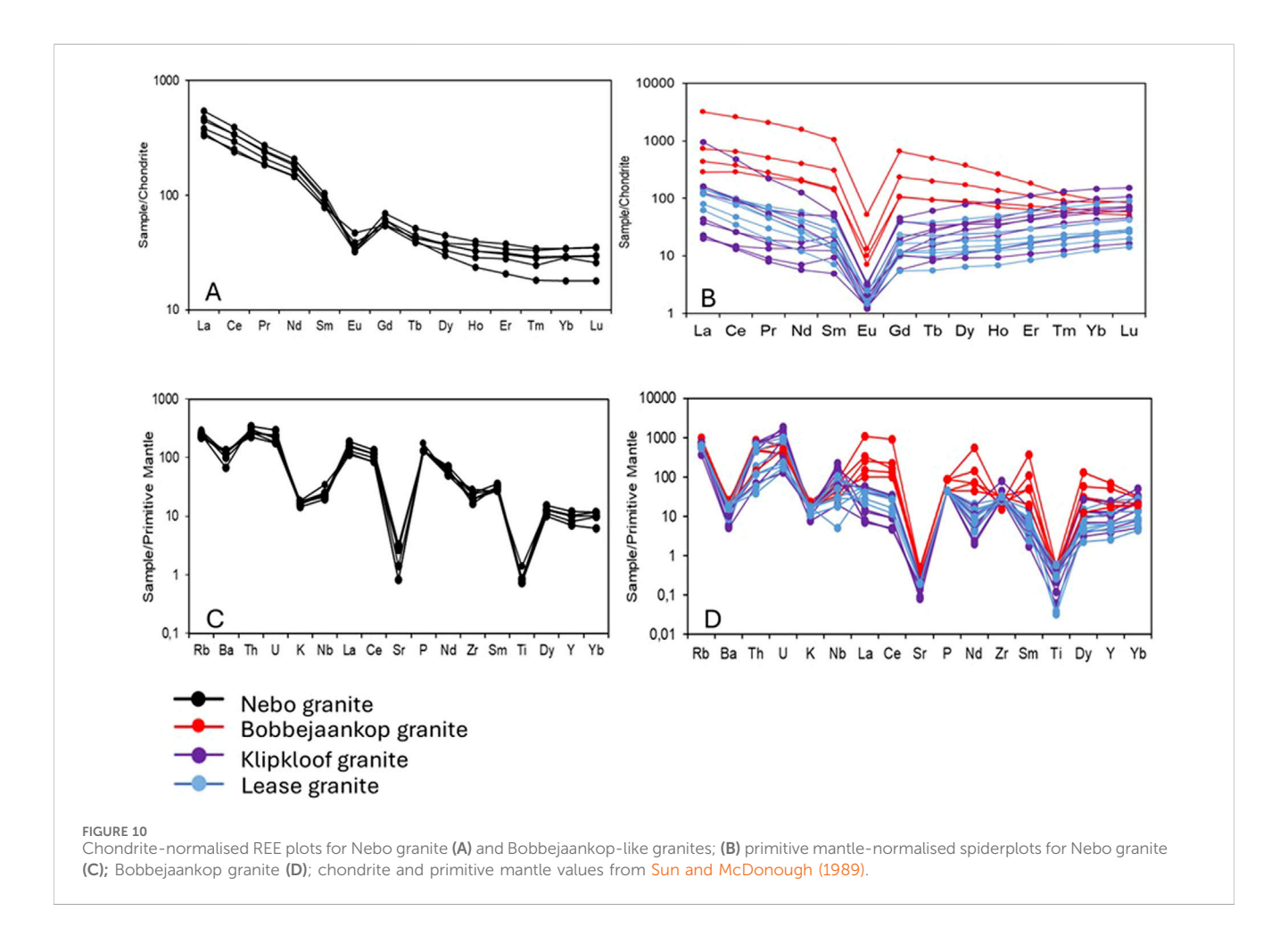
Rare earth elements (REE) and incompatible trace elements in this study were normalised using chondrite and primitive mantle values, respectively (Sun and McDonough, 1989). The REE spidergrams and incompatible trace elements of Nebo and Bobbejaankop-like granite were used to establish the fractionation degrees and possible cogenetic relationship. The differences in characteristics of microgranite, aplitic granite, and medium-to coarse-grained granite within the previously regarded Bobbejaankop-like granite samples are also considered to establish genetic congruency amongst them.

The Nebo granite reflects the general trend of an A-type granite in the REE spidergram (e.g., Hill et al., 1996; Chakhmouradian and Zaitsev, 2012 and references therein) (Figure 10A). The REE pattern for Nebo granite shows a smooth, left-tilted bird's wing enriched in LREE relative to HREE with a negative europium anomaly. The HREE, on the other hand, possesses relatively flat patterns. The negative europium anomalies (Eu/Eu\*) of the Nebo granite samples range between 0.40 and 0.57. The chondrite-normalised values for Nebo granite are invariable; La<sub>n</sub> and Yb<sub>n</sub> range between 330.25 and 538.31 and 17.95 and 35.09. Sm<sub>n</sub> and Gd<sub>n</sub> have chondrite-normalised values of 77.07–103.95 and 53.72–68.86. The ratios of (La/Sm)<sub>n</sub> and (La/Yb)<sub>n</sub> are 4.47–5.17 and 10.14–24.81, respectively.

The REE patterns of the Bobbejaankop granite and associated facies are relatively flat in comparison to the general A-type granite patterns (Figure 10B). The corresponding HREE concentrations in the Bobbejaankop granite and associated microgranite and aplitic facies show enrichment relative to the corresponding LREE compared to the Nebo granite spider-gram. The negative europium anomalies (Eu/Eu\*) of Bobbejaankop granite are relatively large and variable, ranging 0.06–0.23 in comparison with Nebo granite. The La<sub>n</sub> and Yb<sub>n</sub> chondrite-normalised values for Bobbejaankop-like granite samples are noticeably variable, ranging between 19.73 and 961.06 for La<sub>n</sub> and 12.61 and 147.07 for Yb<sub>n</sub>. Sm<sub>n</sub> and Gd<sub>n</sub> range between 4.96 and 1051.88 and 5.49 and 658.17, respectively. Bobbejaankop-like granite samples show La/Sm and La/Yb ratios of 1.14–17.26 and



(A) TEDI versus Rb/Sr binary plot showing the fractionation degrees of the Bobbejaankop-like and the Nebo granite. Nebo granite shows least fractionation, and Bobbejaankop-like granite is relatively more fractionated. (B) Rb (ppm) versus K/Rb plots showing variations of the Nebo granite representing the least differentiated variety and the most differentiated Bobbejaankop-like granite. Historically published data of Nebo granite (H) from Kleemann and Twist (1989) and historical Bobbejaankop granite (H) data from Vonopartis et al. (2020).



0.20–34.80, respectively. Gd/Yb values are 1.59–1.89 and 0.17–7.14 for Nebo and Bobbejaankop granite samples, respectively.

In the enriched HREE wings of the Bobbejaankop-like granite spidergrams, two patterns (two sets) are observed: (1) one set of samples shows a gradual decrease from Gd to Lu and plots above the second set (red patterns in Figure 10B); (2) the second set shows an

increase from Gd to Lu elements (light-blue and purple). The second set is further distinguished into two subsets based on the gradients of their HREE increase: subset (2A) shows a relatively steep increase from Gd to Lu (purple patterns in Figure 10B); subset (2B) shows a steady increase in the same range of HREE (light-blue patterns).

As alluded, set 1 samples stack above set 2 (subset 2A and 2B) in the REE patterns, suggesting higher fractionation trends than the second set. This set also shows larger negative europium anomalies, asserting the higher fractionation degrees. The different REE patterns distinguish the three Bobbejaankop-like granite facies as follows. (1) The main Bobbejaankop facies represented by set 1 and characterised by relatively enriched LREE and corresponding larger Eu/Eu\* observed in RCM 01, RCM02, RCM03, RCM04, and RCM20 samples (red patterns). (2) Microgranitic Klipkloof granitic facies, represented by set 2 (subset 2A), characterised by relatively steep HREE gradients (RCM 05, RCM 11, RCM 14, RCM 16, and RCM 26) (purple patterns). (3) Aplitic Lease granite facies distinguished as part of set 2 (subset 2B) with relatively flat HREE gradients (RCM 06, RCM 07, RCM 16, RCM 20, RCM 21, and RCM 21) (light blue patterns).

The Nebo granite trace elements possess congruent trace element spidergram patterns that are almost superimposed on one another (Figure 10C). Trace element patterns of Bobbejaankop granite, on the other hand, possess contrasting U, Nb, La, Nd, Sm, and Y (i.e., these trace elements show enrichment and depletion of the same trace elements in various samples) in addition to the stacking nature in some corresponding trace elements (Figure 10D). The Nebo and Bobbejaankop granites show trace element patterns akin to upper continental crust source patterns (Rollinson, 1996). The behaviour of the contrasting REE patterns also distinguishes the Bobbejaankop granite from the associated microgranite and aplitic facies according to the subsets described above.

#### 6 Discussion

#### 6.1 Classification of the Bushveld granites

The Nebo and Bobbejaankop granites, together with the associated Klipkloof and Lease facies, possess similar geochemical characteristics. They plot in the same field on various series and tectonic discriminant plots. Major elements of geochemistry affirm their ferroan alkali-type nature, whereas the Shand index categorises them as peraluminous-type of A-type granites. The granites contain lower concentrations of  $P_2O_5$  (<0.04 wt% %), a significant character of fractionated A-type granite as adopted by Kleemann and Twist (1989). The geochemical similarities of various varieties of the Bushveld granites provide a basis for investigating their contemporaneous genetic and fractionation evolution(s).

The Bobbejaankop granite and associated facies possess a wider range (lowest and greatest) of silica content than the Nebo granite. Assuming that both Nebo and Bobbejaankop-like granites are from the same parental magma source and emanated from a single magmatic pulse, the enriched silica Bobbejaankop-like granite samples may suggest that they represent fractionated apical portions. It should follow that the silica-depleted Bobbejaankop-like granite samples should represent a primitive undifferentiated magma phase; however, Nebo granite is regarded as a primitive parental magma phase product (Kleemann and Twist, 1989). Alternatively, the Bobbejaankop-like samples evolved from a different magma pulse more primitive than that which gave rise to the Nebo granite. Application of fractional crystallisation

modelling by either Rayleigh fractionation or least-squares models would be ineffective because the hypothetical pristine Nebo granite samples are mainly superimposed within Bobbejaankop-like granites (Figure 5). Furthermore, the Bobbejaankop-like granites do not exhibit a linear trend from the "pristine" Nebo granite as adopted by Kleemann and Twist (1989) to select parent and daughter samples for modelling. Alternatively, the modal proportion of accessory hornblende minerals is in a range of 5% at most and absent in most cases, whereas an excess of 10% is required for effective Rayleigh fractionation modelling (Kleemann and Twist, 1989; Vonopartis et al., 2020). Additionally, the inferred hydrothermal alteration of the Bobbejaankop-like granite could have destroyed some signatures of magmatic fractionation that would enable linear modelling.

# 6.2 Evidence of fractionation and hydrothermal influence

Trace element geochemistry is employed to distinguish the evolution of granitic melts and their magmatic differentiation trends between the Nebo and Bobbejaankop granites, including the latter's associated Klipkloof and Lease facies. Nebo granite shows relatively low Rb/Sr ratios than the incomparably higher ratios in Bobbejaankop-like granites. Rb is relatively incompatible for Sr, and it partitions more into the melt than solid during crystallisation, resulting in a higher concentration in the residual melt. Alternatively, Ba and Sr are compatible and inherently decrease with increasing fractionation (El Bouseily and El Sokkary, 1975). Consequently, higher Rb/Sr ratios in the Bobbejaankop-like granite may be indicative of its highly fractionated nature relative to Nebo granite. Similarly, the trace element differentiation index (TEDI), defined as Ba  $\times$  (Sr/Rb), considers a product of Ba (barium) with an inverse ratio of Rb and Sr (Walraven, 1986). Ba, like Sr, inherently decreases with increasing fraction. Values less than 10 are indicative of highly fractionated magma products and the influence of magmatic hydrothermal alteration (Bailie, 1997; Freeman, 1998; Bailie and Robb, 2004). As expected, Bobbejaankop-like granites show a range of 0.1-4.0 with respect to ranges between 40 and 399 in Nebo granite (Figure 9A). The use of K/Rb ratios may also discriminate the evolution of granitic melt and fractionation trends (Dostal et al., 2004 and references therein). As generally accepted, Rb increases in the residual melt with concomitant depletion of potassium concentration as it partitions into silicate minerals; hence, the K/Rb ratio decreases with an increasing degree of fractionation (Beus, 1968). The least differentiated granitic magmas tend to have K/Rb ratios of at least 170 (Beus, 1968), whereas the highly differentiated granites often have ratios of less than 150. At times, the lower ratios are not solely attributed to fractionation but also to post-magmatic alterations, such as in hydrothermal environments (Shaw, 1968; Dostal and Chatterjee, 2000). The Nebo granite depicts a K/Rb ratio ranging between 231 and 283, whereas the Bobbejaankop-like granite shows a significantly lower ratio, ranging 69-117. The lower Bobbejaankop-like granite K/Rb ratios suggest higher fractionation and, evidently, the influence of aqueous fluid (Shaw, 1968) (Figure 9B).

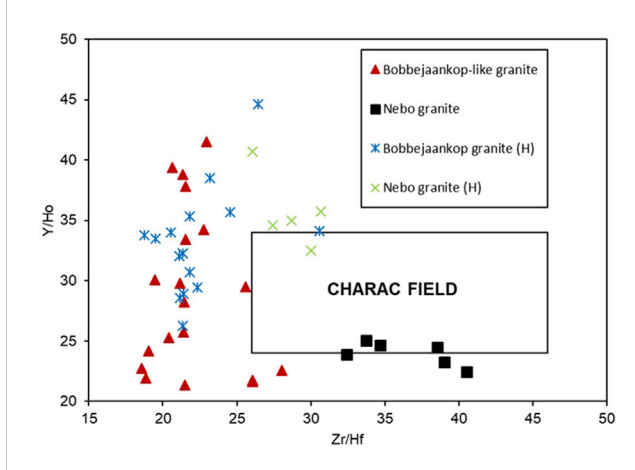


FIGURE 11
Zr/Hf versus Y/Ho diagram of Nebo granite showing CHARAC behaviour and Bobbejaankop-like granites plotting far from the CHARAC-field (after Bau, 1996). Historically published data of Nebo granite (H) sourced from Kleemann and Twist (1989), and historical Bobbejaankop granite (H) data sourced from Vonopartis et al. (2020).

Elemental ratios such as K/Rb, Sr/Rb, and the TEDI discriminant show that Bobbejaankop granite, including its associated Klipkloof and Lease facies, are more fractionated relative to the Nebo granite (Figures 8, 9). They also show coherent and progressive trace-element trends. Furthermore, K/ Rb and TEDI ratios suggest that Bobbejaankop granite and associated facies exhibit a significant degree of magmatichydrothermal alteration in addition to the primary fractionation processes (Shaw, 1968; Dostal and Chatterjee, 2000; Ballouard et al., 2016 and references therein). To augment this assertion, CHArgeand-RAdius-Controlled (CHARAC) trace elements pairs of Y/Ho and Zr/Hf ratios are studied. These ratios are expected to be invariant in a geochemical system owing primarily to their similar charge and radius (Bau, 1996). In the CHARAC-field discriminant by Bau (1996), the Bobbejaankop-like granites plot away from the CHARAC-field, implying an overprinting of fractionation signatures by magmatic-hydrothermal processes (Figure 11). The majority of Zr/Hf ratios in the Bobbejaankoplike granite samples plot below the 25 range, corroborating their relatively high fertility index for (Sn-Mo-W) mineralisation (Bau, 1996). Like the CHARAC pairs, Nb/Ta ratios remain constant in igneous magmatic suites, including comagmatic suites, owing to the similar geochemical character of Nb and Ta (Eby, 1990; Ballouard et al., 2016). In evolving peraluminous magmatic systems, however, Nb is enriched in the residual melt compared to Ta (Linnen and Keppler, 1997). Nebo granite exhibits Nb/Ta ratios of 15.41-21.56 (averaging 16.98, n = 6), whereas the Bobbejaankop and related Klipkloof and Lease granites show lower Nb/Ta ratios ranging 6.46-14.64 (averaging 10.10, n = 19) (Supplementary Table S2). The lower Nb/Ta ratios in the Bobbejaankop and associated granites may signify higher degrees of magmatic fractionation and subsolidus magmatic-hydrothermal processes (cf. Ballouard et al., 2016) (Figure 12).

Chondritic normalised REE geochemistry of Nebo granite shows an enrichment of LREE relative to HREE, with smooth and relatively

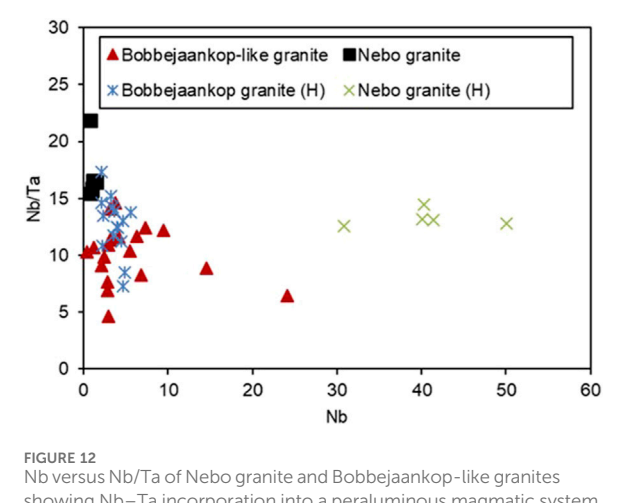


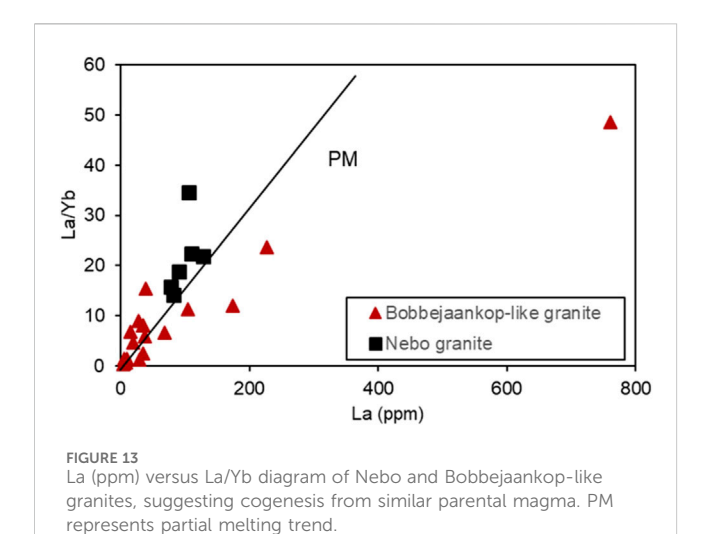
FIGURE 12
Nb versus Nb/Ta of Nebo granite and Bobbejaankop-like granites showing Nb-Ta incorporation into a peraluminous magmatic system. Historically published data of Nebo granite (H) from Kleemann and Twist (1989) and historical Bobbejaankop granite (H) data from Vonopartis et al. (2020).

sharp subduction towards the latter (Figure 9). The europium anomalies (Eu/Eu\*) range between 0.40 and 0.57, implying some degree of fractionation for the LGS suite (Hill et al., 1996). The REE patterns of the Bobbejaankop-like granite discriminate the three granite facies also observed from drill-core and petrographic studies. The main Bobbejaankop granite facies is distinguished by enriched HREE relative to LREE but still maintains the general subduction, although gentle in comparison to the Nebo granite in this study and the general A-type granite observed by Hill et al. (1996). In contrast, the Klipkloof microgranite and aplitic Lease facies exhibit enriched HREE with no evidence of distinction in fractionation disparity between the two in terms of both europium anomalies (Eu/Eu\*) and REE trends. The negative europium anomalies of Bobbejaankop granite facies are larger than both the microgranite and aplitic facies, corroborating the concluded higher degrees of fractionation observed in the latter.

The granites studied have high A/CNK, ranging between 1.58 and 3.67, and are classified as strong-to-hyperaluminous according to the description of peraluminous granites by Clarke (2019). This implies they are oversaturated by alumina contents than the feldspar minerals can accommodate and subsequently form other AFM minerals. Petrographic studies have shown, albeit in minor compositions, the presence of these AFM minerals such as biotite, muscovite, chlorite, and hornblende (Figures 3, 4). Additional mineral assemblages related to the AFM minerals observed encompass saussurite and sericite. A great number of these minerals are hydrous and emphasise strong hydrothermal interference in their petrogenesis.

# 6.3 Evidence of cogenesis and petrogenetic classification

The  $(La/Yb)_n$ ,  $(La/Sm)_n$ , and  $(Gd/Yb)_n$  ratios evaluate the degree of fractionation and post-emplacement hydrothermal activities, and they may decipher petrogenetic sources in granitic suites (Mikkola et al., 2010;



Yusoff et al., 2013). (La/Yb)n, (La/Sm)<sub>n</sub>, and (Gd/Yb)<sub>n</sub> in Nebo granite suggest LREE enrichment relative to HREE compared to Bobbejaankop-like granite samples showing enriched HREE relative to LREE (Figures 10A,B). Generally, the Bobbejaankop-like granite samples show higher (La/Yb)<sub>n</sub> than Nebo granite, affirming that Bobbejaankop granite possesses higher degrees of fractionation, as concluded from Rb/Sr, TEDI, and K/Rb ratios. Furthermore, this (La/Yb)<sub>n</sub> distinguishes the main Bobbejaankop granite from the associated Klipkloof microgranite and aplitic Lease facies. However, all these facies show a relatively linear La (ppm) versus La/Yb evolutionary path, which may suggest a partial melting relationship with varying degrees of fractionation and evolution (Janoušek et al., 2015 and references therein) (Figure 13).

The  $\delta^{18}$ O values of quartz and feldspar can be used to constrain magma source composition in silicic volcanic rocks as they maintain intrinsic character against fractionation, and samples bearing alteration and/or contamination that occur outside the staging chamber can be eliminated (Harris et al., 1997; Fourie and Harris, 2011). Additionally, quartz  $\delta^{18}$ O values provide an effective discriminant amongst granitic plutons such as S-, A- and I-type granites, despite an overlap between the S- and A-type granites. Conversely, feldspar  $\delta^{18}$ O values when applied in conjunction with biotite H-isotopes may indicate magma-fluid interaction and possible mineralogical alteration (Harris et al., 1997; Fourie and Harris, 2011).

This section uses oxygen isotopic data from the literature to augment the current results (Supplementary Table S3). In a single pluton such as LGS, oxygen and hydrogen isotopes from quartz, feldspar, and biotite minerals may discern whether various facies share the same magma source, and any fractionation trends encompass interaction with non-magmatic fluids (Harris et al., 1997). The quartz  $\delta^{18}$ O values obtained from the LGS pluton of the BIC representing the Nebo granite are relatively invariable, averaging  $8.00 \pm 0.81$  ( $1\sigma$ , n = 26) (Fourie and Harris, 2011). Seven samples were selected representing the eastern limb of the pluton, and their recalculated quartz  $\delta^{18}$ O values average  $6.3 \pm 1.1$  ( $1\sigma$ , n = 6) with a range of 4.4–7.5 (Fourie and Harris, 2011; Supplementary Table S3). Samples B39–B41 representing the main eastern limb were extracted from this dataset; all yielded a  $\delta^{18}$ O value of 6.6. These values are comparable with Hill et al. (1996)

from the Sekhukhune Plateau, which is also part of the main eastern limb, with recalculated quartz  $\delta^{18}O$  values averaging 7.9  $\pm$  0.9 (10, n = 7). Both these recalculated quartz  $\delta^{18}O$  values of the main eastern limb are slightly lower than the entire average LGS isotopic values but are relatively invariable. The invariable average  $\delta^{18}O$  values representing the main eastern limb of the LGS suggest they share a genetic parental magma source. The Nebo granite and Bobbejaankop-like facies in this study are also located in the main eastern limb; therefore, it is concluded that they are cogenetic.

The  $\delta^{18}$ O values for feldspar and biotite from the western and eastern limbs of the LGS are relatively inconstant, ranging between 7.4 and 10.2, averaging  $8.64 \pm 1.03$  ( $1\sigma$ , n = 8), and between 1.2 and 9.1, averaging  $2.94 \pm 2.42$  ( $1\sigma$ , n = 9), respectively. Furthermore, the water content for biotite analysed from H-isotopes exceeded the highest expected values generally accepted of 3.5 wt% for biotite, demonstrating substantial chloritization of the ferromagnesian minerals (Fourie and Harris, 2011). Petrographic evidence from the majority of the Nebo granite, Bobbejaankop, and the associated microgranite and aplitic granites portrays various degrees of chloritization of mica, corroborating the H-isotope data. It can therefore be concluded that the variation in both feldspar and biotite  $\delta^{18}$ O values and enriched water content analysed from H-isotopes may represent varying degrees of differentiation and metasomatism of respective samples that once shared a similar magmatic source.

The granites studied show strong-to-hyperaluminous A-type composition (SPAG to HPAG) with geochemical evidence of fractionation and hydrothermal interference. The composition may have resulted from the parental granitic-melt source and/or was generated by indirect processes in the WPG tectonic settings (Clarke, 2019). Peraluminous A-type granite magmas are generated in anhydrous conditions (Clemens et al., 1986; Kleemann and Twist, 1989; Eby, 1990; Bonin, 2007; Frost and Frost, 2011; Mutele and Misra, 2021). However, the current granites exhibit hydrous composition; hence, the parental magma source and/or process(es) responsible for this composition should be construed. Generally, three petrogenetic models are proposed for the generation of parental peraluminous A-type granites magmas: (1) partial melting of the granulites and calc-alkaline granitoids (Clemens et al., 1986; Hill et al., 1996); (2) partial melting of the continental lower crustal material (Whalen et al., 1987); (3) differentiation of the mantle-derived alkaline mafic magma (King et al., 1997). The partial melting model of felsic granulites and calcalkaline granites hypothesis requires a high-temperature and pressure, hydroxyl-free environment (water-undersaturated), and dominant ferromagnesian minerals (Clarke, 2019). In addition, experimental and theoretical calculations show haplogranites to have very low solubility to create excess alumina to attain A/CNK >1.10 ratios (Clarke, 2019 and references therein). The granites studied, however, possess excess alumina, as shown by the presence of hydrous minerals and relatively lower concentrations of CaO and MgO (Figure 6B). Furthermore, the calculated  $\varepsilon_{Nd}$  values of the LGS granites are inconsistent with the crustal values (Fourie and Harris, 2011).

Experimental studies show that partial melting (10%–40%) of continental lower crustal material, particularly with biotite and hornblende composition, at low pressure (4–8 kb) may produce water-deficient peraluminous A-type granites (Creaser et al., 1991;

Patino Douce, 1997). This melt-generation phenomenon is common in subduction and rifting tectonic settings, which contrasts with the WPG settings of the study (Figure 7). Clarke (2019) showed the existence of high-water content in the residual of metapelites after lower degree partial melting, which could be a potential source of hydrous A-type granite. Therefore, it is possible that SPAG/HPAG could represent a product of straight partial melts without the interference of the post-melting processes of this potential source. Nonetheless, dehydration often occurs at relatively low water concentrations (~2% H<sub>2</sub>O), precluding SPAG/HPAG creation from direct partial melting of water-saturated metapelites (Clarke, 2019). Alternatively, the study also demonstrated that direct differentiation of mafic magma could increase the A/CNK ratio, but this process is not feasible for attaining SPAG/HPAG composition (Clarke, 2019). The same study also concluded that the removal of alkalis by subsolidus hydrothermal alteration, in addition to the direct differentiation of mafic magma, could yield SPAG/HPAG composition. The fractionation model, with selective removal of alkalis, best suits the petrographic character of the studied granites due to the presence of AFM-related minerals such as magmatic biotite, muscovite, chlorite, and hornblende, and is corroborated geochemically by high A/CNK ratios. In addition, the Nd isotope data of the coeval RLS are consistent with the granites studied, suggesting that the granite may be derived by the fractional crystallisation of RLS magma (Fourie and Harris, 2011).

#### 7 Conclusion

The geochemistry of the Nebo and Bobbejaankop granites, together with associated porphyritic Klipkloof and aplitic Lease facies, demonstrate characteristics of peraluminous A-type granite. Normalised (La/Yb)n ratios and  $\delta^{18}O$  values, at least within the main eastern limb of the LGS, demonstrate that these granite facies are petrogenetically cogenetic and probably emanate from mantle-derived alkaline mafic magmas genetically related to RLS and developed in WPG tectonic settings. The resulting variation in geochemical compositions is largely a result of varying fractionation degrees and the systematic removal of alkalis by sub-solidus hydrothermal alteration processes in the different facies.

The geochemical variations that exist between the Nebo and Bobbejaankop granites' related facies are distinguished in the following geochemical characteristics.

- 1. The silica contents of the Nebo granite fall within a wider range of the Bobbejaankop granite facies' silica range. Given that these facies are cogenetic, the expectation was that the silica content of the Bobbejaankop granite facies would only be at the greater end (viz., all samples of Bobbejaankop granite-related facies have greater silica content than Nebo) since they are relatively more fractionated. This odd variation may suggest that some parts of the Bobbejaankop represent undifferentiated restite of quartzofeldspathic crystalline rocks, which these suites emanate according to Hill et al. (1996). This variation caused by restite may lead to varied LGS ages of up to 2064 Ma interpreted as antecrysts from initial BIC stages (Skursch et al., 2022).
- 2. Elemental ratios such as K/Rb, Rb/Sr, and TEDI discriminants exhibit variations indicating that Bobbejaankop-like granites

- are more fractionated than the Nebo granite, dispelling any suggestion of contemporaneous evolution. On the contrary, the Bobbejaankop granite and associated microgranite and aplitic facies show coherent and somewhat progressive trace-element trends suggestive of concomitant evolution.
- Chondrite-normalised REE and mantle-normalised trace element variations affirm distinct fractionation evolutionary trends amongst the granite facies.
- 4. Y/Ho-Zr/Hf pairs and Nb/Ta ratios depict variations of both Nebo granite and Bobbejaankop granite-related facies undergoing, respectively, substantial and extensive late magmatic alteration. Furthermore, the Zr/Hf <25 ratios in Bobbejaankop granite and associated Klipkloof and Lease facies indicate high fertility for Sn-W metals.

# Data availability statement

The datasets presented in this study can be found in online repositories. The names of the repository/repositories and accession number(s) can be found in the article/supplementary material.

#### Author contributions

RC: Validation, Data curation, Methodology, Conceptualization, Project administration, Investigation, Writing – review and editing, Writing – original draft, Visualization.

#### **Funding**

The author(s) declare that no financial support was received for the research and/or publication of this article.

## Acknowledgments

The author is indebted to the Council for Geoscience for financial assistance. Paul Nex is thanked for comments on drafts included in the author's dissertation and guidance during fieldwork. Litshedzani Mutele is acknowledged for his constructive criticism in the early versions of the manuscript and valuable guidance during reviews.

# Conflict of interest

The author declares that the research was conducted in the absence of any commercial or financial relationships that could be construed as a potential conflict of interest.

#### Generative AI statement

The author(s) declare that no Generative AI was used in the creation of this manuscript.

Any alternative text (alt text) provided alongside figures in this article has been generated by Frontiers with the support of artificial intelligence and reasonable efforts have been made to ensure accuracy, including review by the authors wherever possible. If you identify any issues, please contact us.

### Publisher's note

All claims expressed in this article are solely those of the authors and do not necessarily represent those of their affiliated

organizations, or those of the publisher, the editors and the reviewers. Any product that may be evaluated in this article, or claim that may be made by its manufacturer, is not guaranteed or endorsed by the publisher.

# Supplementary material

The Supplementary Material for this article can be found online at: https://www.frontiersin.org/articles/10.3389/fgeoc.2025.1640841/full#supplementary-material

### References

Bailie, R. H. (1997). The geology, geochemistry and metallogeny of the felsic rocks of the bushveld complex, north of bronkhorstspruit, South Africa. Johannesburg, South Africa: University of the Witwatersrand, 279. Master of Science dissertation.

Bailie, R. H., and Robb, L. J. (2004). Polymetallic mineralization in the granites of the Bushveld Complex–examples from the central southeastern lobe. *South Afr. J. Geol.* 107, 633–652. doi:10.2113/107.4.633

Ballouard, C., Poujol, M., Boulvais, P., Branquet, Y., Tartèse, R., and Vigneresse, J. L. (2016). Nb-Ta fractionation in peraluminous granites: a marker of the magmatic-hydrothermal transition. *Geology* 44 (3), 231–234. doi:10.1130/g37475.1

Bau, M. (1996). Controls on the fractionation of isovalent trace elements in magmatic and aqueous systems: evidence from Y/Ho, Zr/Hf, and lanthanide tetrad effect. *Contributions Mineralogy Petrology* 123, 323–333. doi:10.1007/s004100050159

Beus, A. A. (1968). Geochemical criteria in theoretical principles of exploration for mineral deposits. Moscow, 127–145.

Bonin, B. (2007). A-type granites and related rocks: evolution of a concept, problems and prospects. *Lithos* 97 (1-2), 1–29. doi:10.1016/j.lithos.2006.12.007

Buick, I. S., Maas, R., and Gibson, R. (2001). Precise U–Pb titanite age constraints on the emplacement of the Bushveld Complex, South Africa. *J. Geol. Soc.* 158 (1), 3–6. doi:10.1144/jgs.158.1.3

Cawthorn, R. G., and Walraven, F. (1998). Emplacement and crystallization time for the Bushveld Complex. *J. Petrology* 39 (9), 1669–1687. doi:10.1093/petroj/39.9.1669

Cawthorn, R. G., Eales, H. V., Walraven, F., Uken, R., and Watkeys, M. K. (2006). "The bushveld complex," in *The geology of South Africa*. Editors M. R. Johnson, C. R. Anhaeusser, and R. J. Thomas (Johannesburg: Council for Geoscience, Geological Society of South Africa), 261–281.

Chakhmouradian, A. R., and Zaitsev, A. N. (2012). Rare earth mineralization in igneous rocks: sources and processes. *Elements* 8 (5), 347–353. doi:10.2113/gselements. 8.5.347

Chauke, R. (2022). Metallogeny of the Boschhoek base Metals occurrence and its geological context with Respect to the Polymetallic mineralization of the Stavoren Fragment of the Bushveld Complex, South Africa. Johannesburg, South Africa: University of the Witwatersrand, 201. Master's thesis.

Clarke, D. B. (2019). The origins of strongly peraluminous granitoid rocks. *Can. Mineralogist* 57 (4), 529–550. doi:10.3749/canmin.1800075

Clemens, J. D., Holloway, J. R., and White, A. J. R. (1986). Origin of an A-type granite; experimental constraints. *Am. mineralogist* 71 (3-4), 317–324.

Coetzee, J., and Twist, D. (1989). Disseminated tin mineralization in the roof of the Bushveld Granite Pluton at the Zaaiplaats Mine, with implications for the genesis of magmatic hydrothermal tin systems. *Econ. Geol.* 84 (7), 1817–1834. doi:10.2113/gsecongeo.84.7.1817

Creaser, R. A., Price, R. C., and Wormald, R. J. (1991). A-type granites revisited: assessment of a residual-source model. *Geology* 19 (2), 163–166. doi:10.1130/0091-7613(1991)019<0163:atgrao>2.3.co;2

Crocker, I. T. (1986). "The Zaaiplaats tinfield, Potgietersrus District," in *Mineral deposits of Southern Africa*. Editors C. R. Anhaeusser, and S. Maske (Johannesburg, South Africa: Geological Society of South Africa), 1287–1299.

Crocker, I. T., Eales, H. V., and Ehlers, D. L. (2001). The fluorite, cassiterite and sulphide deposits associated with the acid rocks of the Bushveld Complex. *Memoir-Geol. Surv. S. Afr. (Pretoria)* 90, 151.

Dostal, J., and Chatterjee, A. K. (2000). Contrasting behaviour of Nb/Ta and Zr/Hf ratios in a peraluminous granitic pluton (Nova Scotia, Canada). *Chem. Geol.* 163 (1-4), 207–218. doi:10.1016/s0009-2541(99)00113-8

Dostal, J., and Shellnutt, J. G. (2016). Origin of peralkaline granites of the Jurassic Bokan Mountain complex (southeastern Alaska) hosting rare metal mineralization. *Int. Geol. Rev.* 58 (1), 1–13. doi:10.1080/00206814.2015.1052995

Dostal, J., Chatterjee, A. K., and Kontak, D. J. (2004). Chemical and isotopic (Pb, Sr) zonation in a peraluminous granite pluton: role of fluid fractionation. *Contributions Mineralogy Petrology* 147 (1), 74–90. doi:10.1007/s00410-003-0547-x

Eby, G. N. (1990). The A-type granitoids: a review of their occurrence and chemical characteristics and speculations on their petrogenesis. *Lithos* 26 (1-2), 115–134. doi:10. 1016/0024-4937(90)90043-z

El Bouseily, A. M., and El Sokkary, A. A. (1975). The relation between Rb, Ba and Sr in granitic rocks. *Chem. Geol.* 16 (3), 207–219. doi:10.1016/0009-2541(75)90029-7

Eriksson, P. G., Reczko, B. F., Jaco Boshoff, A., Schreiber, U. M., Van der Neut, M., and Snyman, C. P. (1995). Architectural elements from Lower Proterozoic braid-delta and high-energy tidal flat deposits in the Magaliesberg Formation, Transvaal Supergroup, South Africa. *Sediment. Geol.* 97 (1-2), 99–117. doi:10.1016/0037-0738(95)00004-r

Eriksson, P. G., Altermann, W., Hartzer, F. J., Johnson, M. R., Anhaeusser, C. R., and Thomas, R. J. (2006). The Transvaal Supergroup and its precursors. *Geol. S. Afr.*, 237–260

Evans, R. (2015). The nature, structural style, and origin of IOCG-style mineralization at Boschhoek in the felsic rocks of the Bushveld Complex, South Africa, Master of Earth Sciences project. United Kingdom: University of Oxford, 110.

Ferré, E. C., Wilson, J., and Gleizes, G. (1999). Magnetic susceptibility and AMS of the Bushveld alkaline granites, South Africa. *Tectonophysics*, 307 (1–2), 113–133. doi:10. 1016/S0040-1951(99)00122-5

Fourie, D. S., and Harris, C. (2011). O-isotope study of the Bushveld Complex granites and granophyres: constraints on source composition, and assimilation. *J. Petrology* 52 (11), 2221–2242. doi:10.1093/petrology/egr045

Freeman, L. A. (1998). The nature of hydrothermal fluids associated with granite-hosted, polymetallic mineralisation in the eastern lobe of the Bushveld Complex. Johannesburg, South Africa: University of the Witwatersrand, 333. Doctoral thesis.

Frost, B. R., and Frost, C. D. (2008). A geochemical classification for feldspathic igneous rocks. *J. Petrology* 49 (11), 1955–1969. doi:10.1093/petrology/egn054

Frost, C. D., and Frost, B. R. (2011). On ferroan (A-type) granitoids: their compositional variability and modes of origin. *J. petrology* 52 (1), 39–53. doi:10. 1093/petrology/egq070

Frost, B. R., Barnes, C. G., Collins, W. J., Arculus, R. J., Ellis, D. J., and Frost, C. D. (2001). A geochemical classification for granitic rocks. *J. petrology* 42 (11), 2033–2048. doi:10.1093/petrology/42.11.2033

Gough, D. I., and Van Niekerk, C. B. (1959). A study of the palaeomagnetism of the bushveld gabbrot. *Philos. Mag.* 4 (37), 126-136. doi:10.1080/14786435908238231

Harmer, R. E., and Armstrong, R. A. (2000). New precise dates on the acid phase of the Bushveld and their implications. Abstract. Workshop on the Bushveld Complex, 18th-21st November 2000, Burgersfort. Johannesburg: University of Witwatersrand.

Harris, C., Faure, K., Diamond, R. E., and Scheepers, R. (1997). Oxygen and hydrogen isotope geochemistry of S-and I-type granitoids: the Cape Granite suite, South Africa. *Chem. Geol.* 143 (1-2), 95–114. doi:10.1016/s0009-2541(97)00103-4

Hill, M., Barker, F., Hunter, D., and Knight, R. (1996). Geochemical characteristics and origin of the Lebowa granite suite, Bushveld Complex. *Int. Geol. Rev.* 38 (3), 195–227. doi:10.1080/00206819709465331

Irvine, T. N., and Baragar, W. R. A. F. (1971). A guide to the chemical classification of the common volcanic rocks. *Can. J. Earth Sci.* 8 (5), 523–548. doi:10.1139/e71-055

Janoušek, V., Moyen, J. F., Martin, H., Erban, V., and Farrow, C. (2015). Geochemical modelling of igneous processes: principles and recipes in R language. Springer.

Kamaunji, V. D., Wang, L. X., Chen, W., Girei, M. B., Ahmed, H. A., Zhu, Y. X., et al. (2024). Petrogenesis and rare-metal mineralization of the Ririwai alkaline granitoids, north-central Nigeria: mineralogical and geochemical constraints. *Int. Geol. Rev.* 66 (13), 2409–2439. doi:10.1080/00206814.2023.2283875

- King, P. L., White, A. J. R., Chappell, B. W., and Allen, C. M. (1997). Characterization and origin of aluminous A-type granites from the Lachlan Fold Belt, southeastern Australia. *J. Petrology* 38 (3), 371–391. doi:10.1093/petroj/38.3.371
- Kinnaird, J. A., Bowden, P. L., Ixer, R. A., and Odling, N. W. A. (1985). Mineralogy, geochemistry and mineralization of the Ririwai complex, northern Nigeria. *J. Afr. Earth Sci.* 3 (1-2), 185–222. doi:10.1016/0899-5362(85)90036-3
- Kinnaird, J. A., Kruger, F. J., and Cawthorn, R. G. (2004). Rb-Sr and Nd-Sm isotopes in fluorite related to the granites of the Bushveld Complex. *South Afr. J. Geol.* 107 (3), 413–430. doi:10.2113/107.3.413
- Kleemann, G. J. (1985). The geochemistry and petrology of the roofrocks of the Bushveld Complex east of groblersdal. Pretoria, South Africa: University of Pretoria. Doctoral dissertation
- Kleemann, G. J., and Twist, D. (1989). The compositionally-zoned sheet-like granite pluton of the Bushveld Complex: evidence bearing on the nature of A-type magmatism. *J. Petrology* 30 (6), 1383–1414. doi:10.1093/petrology/30.6.1383
- Labuschagne, L. S. (2004). Evolution of the ore-forming fluids in the Rooiberg tin field, 96. South Africa: Council for Geoscience, 126.
- Linnen, R. L., and Keppler, H. (1997). Columbite solubility in granitic melts: consequences for the enrichment and fractionation of Nb and Ta in the Earth's crust. *Contributions Mineralogy Petrology* 128 (2), 213–227. doi:10.1007/s004100050304
- MacCaskie, D. R. (1983). Differentiation of the Nebo granite (Main Bushveld Granite), South Africa. Oregon, United States: University of Oregon. Unpublished PhD thesis
- Maniar, P. D., and Piccoli, P. M. (1989). Tectonic discrimination of granitoids. *Geol. Soc. Am. Bull.* 101 (5), 635–643. doi:10.1130/0016-7606(1989)101<0635: tdog>2.3.co;2
- McNaughton, N. J., Pollard, P. J., Groves, D. I., and Taylor, R. G. (1993). A long-lived hydrothermal system in Bushveld granites at the Zaaiplaats tin mine; lead isotope evidence. *Econ. Geol.* 88 (1), 27–43. doi:10.2113/gsecongeo.88.1.27
- Mikkola, P., Kontinen, A., Huhma, H., and Lahaye, Y. (2010). Three Paleoproterozoic A-type granite intrusions and associated dykes from Kainuu, East Finland. *Bull. Geol. Soc. Finl.* 82 (2), 81–100. doi:10.17741/bgsf/82.2.002
- Molyneux, T. G., and Klinkert, P. S. (1978). A structural interpretation of part of the eastern mafic lobe of the Bushveld Complex and its surrounds. *South Afr. J. Geol.* 81 (3), 359–368.
- Mutele, L., and Hunt, J. P. (2022). Investigation of hydrothermally altered "Mantos" zones in granites of the southwestern Bushveld complex, South Africa: insight into their mode of formation and F-REE mineralisation. *J. Afr. Earth Sci.* 194, 104629. doi:10. 1016/j.jafrearsci.2022.104629
- Mutele, L., and Misra, S. (2021). Geochemical evolution of the Lebowa granite pluton in western Bushveld igneous complex, South Africa: more insight into the evolution of bimodal a-type granitoid. *Geol. J.* 56 (7), 3557–3583. doi:10.1002/gj.4117
- Ollila, J. T. (1981). A fluid inclusion and mineralogical study of tin deposits and rocks associated with the bushveld complex at the zaaiplaats, rooiberg and union tin mines in the Central transvaal, South Africa. Johannesburg: Rand Afrikaans University, 257. Ph.D. thesis.
- Patiño Douce, A. E. (1997). Generation of metaluminous A-type granites by low-pressure melting of calc-alkaline granitoids. Geology 25 (8), 743–746. doi:10.1130/0091-7613(1997)025<0743:gomatg>2.3.co;2
- Pearce, J. A., Harris, N. B., and Tindle, A. G. (1984). Trace element discrimination diagrams for the tectonic interpretation of granitic rocks. *J. Petrology* 25 (4), 956–983. doi:10.1093/petrology/25.4.956
- Pollard, P. J., and Taylor, R. G. (1986). Progressive evolution of alteration and tin mineralization; controls by interstitial permeability and fracture-related tapping of magmatic fluid reservoirs in tin granites. *Econ. Geol.* 81 (7), 1795–1800. doi:10.2113/gsecongeo.81.7.1795
- Pollard, P. J., Taylor, R. G., and Tate, N. M. (1989). Textural evidence for quartz and feldspar dissolution as a mechanism of formation for maggs pipe, zaaiplaats tin mine, South Africa. *Miner. deposita* 24 (3), 210–218. doi:10.1007/bf00206444
- Pollard, P. J., Andrew, A. S., and Taylor, R. G. (1991). Fluid inclusion and stable isotope evidence for interaction between granites and magmatic hydrothermal fluids during formation of disseminated and pipe-style mineralization at the zaaiplaats tin mine. *Econ. Geol.* 86 (1), 121–141. doi:10.2113/gsecongeo.86.1.121
- Robb, L. J., Robb, V. M., and Walraven, F. (1994). The albert silver mine revisited; toward a model for polymetallic mineralization in granites of the bushveld Complex, South Africa. *Explor. Min. Geol.* 3 (3), 247–262.

- Robb, L. J., Freeman, L. A., and Armstrong, R. A. (2000). Nature and longevity of hydrothermal fluid flow and mineralisation in granites of the bushveld complex, South Africa. *Earth Environ. Sci. Trans. R. Soc. Edinb.* 91 (1-2), 269–281. doi:10.1017/s0263593300007434
- Rollinson, H. R. (1996). Tonalite-trondhjemite-granodiorite magmatism and the genesis of Lewisian crust during the Archaean. *Geol. Soc. Lond. Spec. Publ.* 112 (1), 25–42. doi:10.1144/gsl.sp.1996.112.01.02
- Rozendaal, A., Toros, M. S., and Anderson, J. R. (1986). "The rooiberg tin deposits, west-central transvaal," in *Mineral deposits of Southern Africa*, 1307–1327.
- Rozendaal, A., Misiewicz, J. E., and Scheepers, R. (1995). The tin zone: sediment-hosted hydrothermal tin mineralization at rooiberg, South Africa. *Miner. Deposita* 30 (2), 178–187. doi:10.1007/bf00189347
- SACS (South African Committee for Stratigraphy) (1980). in Stratigraphy of South Africa. Part 1: lithostratigraphy of the Republic of South Africa, south west africa/namibia and the republics of bophuthatswana, transkei, and Venda. Editor Kent, L. E. (Pretoria, South Africa: Handbook Geological Survey of South Africa).
- Scoates, J. S., Wall, C. J., Friedman, R. M., Weis, D., Mathez, E. A., and VanTongeren, J. A. (2021). Dating the bushveld complex: timing of crystallization, duration of magmatism, and cooling of the world's largest layered intrusion and related rocks. *J. Petrology* 62 (2), egaa107. doi:10.1093/petrology/egaa107
- Scoggins, A. J. (1991). Kwandebele: a regional appraisal of the base metal potential of the bushveld granites. *STK Mineral. Dev. Div.* LIB REF No: 2958.
- Shand, S. J. (1922). The problem of the alkaline rocks. Proc. Geol. Soc. S. Afr. 25, 19-33.
- Shaw, D. M. (1968). A review of K-Rb fractionation trends by covariance analysis. Geochimica Cosmochimica Acta 32 (6), 573–601. doi:10.1016/0016-7037(68)90050-1
- Skursch, O., Corfu, F., Tegner, C., Lesher, C. E., Andreasen, R., Hagen-Peter, G. A., et al. (2022). Zircon U–Pb chronology and Hf isotopes of the Lebowa Granite Suite and petrogenesis of the Bushveld Complex, South Africa. *Contributions Mineralogy Petrology* 177 (2), 26. doi:10.1007/s00410-022-01889-7
- Smits, G. (1979). A mineralogical investigation of the Rooibokkop-Boschhoek hydrothermal copper deposit, northeast of Marble Hall, Transvaal. Master of Science thesis. Pretoria, South Africa: University of Pretoria, 156.
- Stear, W. M. (1977). The stratabound tin-deposits and structure of the Rooiberg Fragment. South Afr. J. Geol. 80 (2), 67–78.
- Sun, S. S., and McDonough, W. F. (1989). Chemical and isotopic systematics of oceanic basalts: implications for mantle composition and processes. *Geol. Soc. Lond. Spec. Publ.* 42 (1), 313–345. doi:10.1144/gsl.sp.1989.042.01.19
- Vonopartis, L., Nex, P., Kinnaird, J., and Robb, L. (2020). Evaluating the changes from endogranitic magmatic to magmatic-hydrothermal mineralization: the zaaiplaats tin granites, bushveld Igneous complex, South Africa. *Minerals* 10 (4), 379. doi:10.3390/min10040379
- Wagner, P. A. (1921). *The Mutue Fides-stavoren Tin fields*, 16. Memoir: Geological Survey of South Africa, 191.
- Walraven, F. (1986). Stratigraphy and structure of the Nebo granite, bushveld complex, South Africa. Abstr. Geocongress' 86. Geol. Soc. S. Afr., 637–642.
- Whalen, J. B., Currie, K. L., and Chappell, B. W. (1987). A-type granites: geochemical characteristics, discrimination and petrogenesis. *Contributions mineralogy petrology* 95 (4), 407–419. doi:10.1007/bf00402202
- Whalen, J. B., Jenner, G. A., Longstaffe, F. J., Robert, F., and Gariépy, C. (1996). Geochemical and isotopic (O, Nd, Pb and sr) constraints on A-type granite petrogenesis based on the Topsails igneous suite, Newfoundland Appalachians. *J. Petrology* 37 (6), 1463–1489. doi:10.1093/petrology/37.6.1463
- Wilson, J., Ferré, E. C., and Lespinasse, P. (2000). Repeated tabular injection of high-level alkaline granites in the eastern Bushveld, South Africa. *J. Geol. Soc.* 157 (5), 1077–1088. doi:10.1144/jgs.157.5.1077
- Yusoff, Z. M., Ngwenya, B. T., and Parsons, I. (2013). Mobility and fractionation of REEs during deep weathering of geochemically contrasting granites in a tropical setting, Malaysia. *Chem. Geol.* 349-350, 71–86. doi:10.1016/j.chemgeo.2013.04.016
- Zeh, A., Ovtcharova, M., Wilson, A. H., and Schaltegger, U. (2015). The Bushveld Complex was emplaced and cooled in less than one million years—results of zirconology, and geotectonic implications. *Earth Planet. Sci. Lett.* 418, 103–114. doi:10.1016/j.epsl. 2015.02.035
- Zeh, A., Wilson, A. H., and Ovtcharova, M. (2016). Source and age of upper Transvaal Supergroup, South Africa: age-Hf isotope record of zircons in magaliesberg quartzite and dullstroom lava, and implications for Paleoproterozoic (2.5–2.0 Ga) continent reconstruction. *Precambrian Res.* 278, 1–21. doi:10.1016/j.precamres.2016.03.017